

1 **Classification:** Biological Sciences with a minor category of Cell Biology

2

3 **Title:** Long non-coding RNA *GRASLND* enhances chondrogenesis via suppression of interferon  
4 type II signaling pathway

5 **Authors:** Nguyen P.T. Huynh<sup>a,b,c,d</sup>, Catherine C. Gloss<sup>a,b,d</sup>, Jeremiah Lorentz<sup>a,b,d</sup>, Ruhang  
6 Tang<sup>a,b,d</sup>, Jonathan M. Brunger<sup>e</sup>, Audrey McAlinden<sup>a,b,d</sup>, Bo Zhang<sup>d</sup>, Farshid Guilak<sup>a,b,d</sup>

7

8 **Short title:** LncRNA *GRASLND* suppresses IFN to enhance chondrogenesis

9

10 **Author Affiliation:**

11 a. Department of Orthopaedic Surgery, Washington University in St Louis, MO, USA, 63110

12 b. Shriners Hospitals for Children – St. Louis, St. Louis, MO, USA, 63110

13 c. Department of Cell Biology, Duke University, NC, USA, 27708

14 d. Center of Regenerative Medicine, Washington University in St Louis, MO, USA, 63110

15 e. Department of Cellular and Molecular Pharmacology, University of California, San Francisco,  
16 CA, USA, 94158

17

18

19 **Corresponding Author:**

20 Farshid Guilak

21 Campus Box 8233

22 McKinley Research Building, Room 3121

23 St Louis, MO, USA, 63110

24 Email Address: [guilak@wustl.edu](mailto:guilak@wustl.edu)

25

26 **Keywords:** mesenchymal stem cells, tissue engineering, regenerative medicine,  
27 **RNF144A-AS1**

28

1 **Abstract**

2 Long non-coding RNAs (lncRNAs) play critical roles in regulating gene expression and  
3 cellular processes; however, their roles in musculoskeletal development, disease, and  
4 regeneration remain poorly understood. Here, we identified a novel lncRNA, Glycosaminoglycan  
5 Regulatory ASSociated Long Non-coDing RNA (*GRASLND*) as a regulator of mesenchymal  
6 stem cell (MSC) chondrogenesis, and we investigated its basic molecular mechanism and its  
7 potential application towards regenerative medicine. *GRASLND*, a primate-specific lncRNA, is  
8 upregulated during MSC chondrogenesis and appears to act directly downstream of SRY-Box 9  
9 (SOX9), but not Transforming Growth Factor Beta 3 (TGF- $\beta$ 3). Utilizing the established model of  
10 pellet formation for MSC chondrogenesis, we showed that the silencing of *GRASLND* resulted  
11 in lower accumulation of cartilage-like extracellular matrix, while *GRASLND* overexpression,  
12 either via transgene ectopic expression or by endogenous activation via CRISPR, significantly  
13 enhanced cartilage matrix production. *GRASLND* acts to inhibit interferon gamma (IFN- $\gamma$ ) by  
14 binding to Eukaryotic Initiation Factor-2 Kinase EIF2AK2. We further demonstrated that  
15 *GRASLND* exhibits a protective effect in engineered cartilage against interferon type II across  
16 different sources of chondroprogenitor cells. Our results indicate an important role of *GRASLND*  
17 in regulating stem cell chondrogenesis, as well as its therapeutic potential in the treatment of  
18 cartilage-related diseases, such as osteoarthritis.

19

1 **Significance**

2 Long non-coding RNAs (lncRNAs) play critical roles in gene regulation and cellular  
3 physiology; however, the role of lncRNAs in controlling stem cell chondrogenesis remains to be  
4 determined. Here, we utilized next generation sequencing of adult stem cell chondrogenesis to  
5 identify a set of potential lncRNA candidates involved in this process. We identified lncRNA  
6 Glycosaminoglycan Regulatory ASsociated Long Non-coDing RNA (*GRASLND*) and  
7 characterized its molecular mechanism of action. We described a novel role of *GRASLND* in  
8 positive regulation of chondrogenesis via its inhibition of type II interferon. Importantly, we  
9 showed that overexpression of *GRASLND* augments stem cell chondrogenesis, providing a  
10 promising approach to enhancing stem cell chondrogenesis and cartilage regeneration.

11

1 **/body**

2 ***Introduction***

3 Articular cartilage is an aneural, avascular tissue and has little or no capacity for intrinsic  
4 repair (1). While there are currently no effective treatments available for cartilage repair, focal  
5 cartilage or osteochondral lesions generally progress to osteoarthritis (OA), a progressive  
6 degenerative disease characterized by changes in the articular cartilage and remodeling of  
7 other joint tissues such as the synovium and subchondral bone. Thus, there remains an  
8 important need for regenerative therapies that can enhance cartilage repair through tissue  
9 engineering or cell therapy approaches (2-7).

10 In this regard, adult stem cells such as bone marrow derived mesenchymal stem cells  
11 (MSCs) or adipose-derived stem cells (ASCs) provide a readily accessible source of multipotent  
12 cells that show significant promise for regenerative medicine (8-11). When cultured in a defined  
13 cocktail supplemented with Transforming Growth Factor Beta 3 (TGF- $\beta$ 3), MSCs produce a  
14 cartilaginous matrix that is rich in glycosaminoglycan (GAG) and collagen type II (COLII) (12,  
15 13). However, the complete pathway involved in MSC chondrogenesis is not fully deciphered,  
16 and a detailed understanding of the gene regulatory networks that control this process could  
17 provide new insights that accelerate and improve cartilage regeneration from endogenous or  
18 exogenously grafted MSCs.

19 Increasing evidence suggests that such gene regulatory pathways operational in stem cell  
20 differentiation may rely not only on protein-coding RNAs, but also on non-coding RNAs  
21 (ncRNAs). Non-coding RNAs (ncRNAs) were initially difficult to identify because they neither  
22 possessed open reading frames, nor were they evolutionarily highly conserved (14). In one of  
23 the first landmark studies, chromatin-state mapping was used to identify transcriptional units of  
24 functional large intervening non-coding RNAs (lincRNAs) that were actively transcribed in  
25 regions flanking protein-coding loci (15), and follow-up loss-of-function studies indicated that



1 these lincRNAs were indeed crucial for the maintenance of pluripotency in embryonic stem cells  
2 (16). There is a growing understanding of long non-coding RNA (lncRNA) function in a multitude  
3 of tissues and cellular processes. For example, detailed mechanistic studies on the role of  
4 lncRNAs in X chromosome inactivation (17), or nervous system development and functions (18,  
5 19) have been previously reported. However, knowledge of their roles in the musculoskeletal  
6 system, particularly in chondrogenesis remains limited. Only a handful of functional studies have  
7 been carried out in this regard. For example, lncRNA-HIT (HOXA Transcript Induced by TGF $\beta$ )  
8 (20) has been shown to play a role in epigenetic regulation during early limb development.  
9 Other studies have implicated a specific lncRNA, ROCR (Regulator of Chondrogenesis RNA)  
10 (21), to act upstream of SRY-Box 9 (SOX9) and regulate chondrocyte differentiation (22).

11 As one of their many modes of actions, lncRNAs are also known to regulate and modulate  
12 various signaling cascades involved in the control of gene regulatory networks. Therefore, there  
13 may exist a connection between lncRNA candidates and signaling pathways previously known  
14 to play a role in the musculoskeletal system development. More specifically, there is growing  
15 evidence for the role of interferon (IFN) in skeletal tissue development and homeostasis (23-31).  
16 There are two main types of IFN. Type I includes mainly IFN alpha (IFN- $\alpha$ ) and IFN beta (IFN- $\beta$ )  
17 that form complexes with Interferon Alpha and Beta Receptors (IFNARs), activating the Janus  
18 Kinase/ Signal Transducers and Activators of Transcription (JAK/STAT) pathway by  
19 phosphorylation of STAT1 (Signal Transducer and Activator of Transcription 1) and STAT2  
20 (Signal Transducer and Activator of Transcription 2). Phosphorylated STAT1/STAT2 then form  
21 complexes with IRF9 (IFN Regulatory Factor 9) and translocate into the nucleus to activate  
22 downstream targets via the interferon-stimulated responsible element (ISRE) DNA binding motif.  
23 Type II, on the other hand, relies on activation of the JAK/STAT pathway following the binding of  
24 IFN gamma (IFN- $\gamma$ ) to Interferon Gamma Receptors (IFNGRs). This subsequently results in the  
25 phosphorylation and dimerization of STAT1 that translocates into the nucleus and induces  
26 downstream targets via the gamma activated sequence (GAS) DNA binding element (32-34).

1 Although interferons (IFN) are widely known for their antiviral response, they can also act in  
2 other aspects of cellular regulation (33). Interestingly, IFN- $\gamma$  has been implicated in non-viral  
3 processes, most notably its priming effect in auto-immune diseases such as lupus nephritis,  
4 multiple sclerosis, or rheumatoid arthritis (35). An additional goal of this study was to elucidate  
5 the link between IFN- $\gamma$  and our lncRNA candidate, and how this interaction could potentially play  
6 a role in MSC chondrogenesis and cartilage tissue engineering.

7 In a recent publication, we used high-depth RNA sequencing to map the transcriptomic  
8 trajectory of MSC chondrogenesis (36). This dataset provides a unique opportunity to identify  
9 candidate genes for subsequent functional characterization as regulators of chondrogenesis.  
10 Here, we used bioinformatic approaches to integrate our RNA-seq data with other publicly  
11 available datasets, applying a rational and systematic data mining method to define a  
12 manageable list of final candidates for follow-up experiments. As a result, we identified  
13 *RNF144A-AS1* to be a crucial regulator of chondrogenesis, and proposed the name  
14 Glycosaminoglycan Regulatory ASsociated Long Non-coDing RNA (*GRASLND*). We showed  
15 that *GRASLND* enhances chondrogenesis by acting to suppress the IFN- $\gamma$  signaling pathway,  
16 and this effect was prevalent across different adult stem cell types and conditions. Together,  
17 these results highlight novel roles of *GRASLND* and its modulation of IFN in stem cell  
18 chondrogenesis, as well as its therapeutic potential to enhance cartilage regeneration.

## 19 **Results**

### 20 ***RNF144A-AS1* is crucial to and specifically upregulated in chondrogenesis**

21 First, we utilized our published database on MSC chondrogenesis (GSE109503) (36) to  
22 identify long non-coding RNA candidates. We investigated the expression patterns of MSC  
23 markers (*ALCAM*, *ENG*, *VCAM1*), chondrogenic markers (*ACAN*, *COL2A1*, *COMP*), and SOX  
24 transcription factors (*SOX5*, *SOX6*, *SOX9*) (Figure S1A). Pearson correlation analysis revealed  
25 141 lncRNAs whose expression was highly correlated to those of MSC markers, 40 lncRNAs to

1 chondrogenic markers, and 17 lncRNAs to SOX transcription factors (Figure S1B, C). Among  
2 those, two were downregulated and two were upregulated upon ectopic SOX9 overexpression  
3 (Table 1) (GSE69110) (37). To validate their functions in chondrogenesis, we systematically  
4 designed small hairpin RNAs (shRNAs) targeting each candidate and assessed knockdown  
5 effect after 21 days of chondrogenic induction. We successfully designed two target shRNAs for  
6 each of three candidates, and one target shRNA for the other candidate (Figure S2). We  
7 showed that knockdown of two out of three MSC-related lncRNAs did not influence the  
8 production of glycosaminoglycans (GAG) - an important extracellular matrix component in  
9 cartilage (Figure S2). While these lncRNAs may have other regulatory functions in MSCs, their  
10 roles in chondrogenesis appeared to be minimal. Moreover, we found that lower levels of MSC-  
11 correlated lncRNAs did not prime the MSCs toward chondrogenesis. However, knockdown of  
12 *RNF144A-AS1* (*RNF144A Antisense RNA 1*) resulted in decreased expression of chondrogenic  
13 markers (*COL2A1*, *ACAN*), and upregulation of apoptotic (*CASP3*) and cellular senescence  
14 (*TP53*) markers (Figure 1A, B). This effect was not due to nonspecific cytotoxicity of examined  
15 shRNAs, as released levels of lactate dehydrogenase (LDH) were similar among control and  
16 shRNA-expressing cells (Figure S3). In addition, biochemical assays indicated a reduction in  
17 GAG deposition ( $p < 0.0001$ ) as well as DNA and GAG/DNA levels ( $p < 0.001$ ) (Figure 1 C-E).  
18 Histologically, we observed the same phenotypic loss of GAG and collagen type II in the  
19 extracellular matrices (ECM) of pellet samples with *RNF144A-AS1* targeted shRNAs, while the  
20 scrambled controls displayed explicit staining of these proteins (Figure 1F). Taken together, this  
21 data indicates that *RNF144A-AS1* may be required for both cellular proliferation and cartilage-  
22 like matrix production.

23 To establish whether *RNF144A-AS1* expression is specific to chondrogenesis or involved in  
24 other differentiation pathways, MSCs were induced towards adipogenic, osteogenic, or  
25 chondrogenic lineages, and *RNF144A-AS1* expression was measured at various timepoints  
26 throughout these processes. Successful differentiation was observed with an increase in

1 lineage-specific markers: *PPARG* (*Peroxisome Proliferator Activated Receptor Gamma*) and  
2 *ADIPOQ* (*Adiponectin, C1Q And Collagen Domain Containing*) for adipogenesis, *COL1A1*  
3 (*Collagen Type I Alpha 1 Chain*) and *COL10A1* (*Collagen Type X Alpha Chain 1*) for  
4 osteogenesis, and *ACAN* (*Aggrecan*), *SOX9* (*SRY-Box 9*) and *COL2A1* (*Collagen Type II Alpha*  
5 *Chain 1*) for chondrogenesis (Figure 1 G-I). We found that *RNF144A-AS1* expression was  
6 particularly enriched as chondrogenesis progressed (Figure 1I). In contrast, *RNF144A-AS1*  
7 peaked at earlier timepoints during adipogenesis but decreased at later time points (Figure 1G),  
8 and downregulated when MSCs underwent osteogenic induction (Figure 1H), indicating that  
9 *RNF144A-AS1* is specifically upregulated in chondrogenesis. Furthermore, we speculate that  
10 *RNF144A-AS1* may display inhibitory effects on osteogenesis and adipogenesis, thus being  
11 downregulated during these processes.

12 To validate these gene expression findings, we performed RNA fluorescence *in situ*  
13 hybridization (FISH) throughout the time course of MSC chondrogenesis. Pellets exhibited  
14 *RNF144A-AS1* FISH signals at later time points during chondrogenic differentiation, consistent  
15 with RNA-seq data (Figure 2A). Next, to confirm *RNF144A-AS1* subcellular location, we  
16 performed qRT-PCR on isolated nuclear and cytoplasmic fractions of day 21 MSC pellets  
17 (Figure 2B). We compared the subcellular expression patterns of *RNF144A-AS1* to *NEAT1*  
18 (*Nuclear Paraspeckle Assembly Transcript 1*) and *GAPDH* (*Glyceraldehyde 3-Phosphate*  
19 *Dehydrogenase*). *NEAT1* is a lncRNA previously characterized to localize to the nucleus (38,  
20 39), and *GAPDH* is an mRNA and thus should be exported to the cytoplasm for protein  
21 synthesis. Consistent with previous findings, *NEAT1* displayed lower expression in the  
22 cytoplasmic compared to the nuclear fraction, in contrast to *GAPDH*. By this measurement,  
23 *RNF144A-AS1* exhibited higher expression in the cytoplasm, indicating its cytoplasmic  
24 subcellular location. Our finding was recapitulated by RNA *in situ* hybridization followed by  
25 confocal microscopy (Figure 2C). Interestingly, since *RNF144A-AS1* showed punctate labeling,  
26 we speculate that this lncRNA may function in the form of an RNA-protein complex.

## 1 **Characterization of *RNF144A-AS1***

2 We examined the characteristics of *RNF144A-AS1* by first exploring its evolutionary  
3 conservation. Except for exon 1, the genomic region of *RNF144A-AS1* is highly conserved in  
4 primates (*Homo sapiens*, *Pan troglodytes*, and *Rhesus macaque*) whose common ancestor  
5 traced back to 25 million years ago (40), while sequences are less conserved in other mammals  
6 (Figure 3A). This suggests that *RNF144A-AS1* may belong to a group of previously identified  
7 primate-specific lncRNAs (41, 42).

8 Per GENCODE categorization, the AS (antisense) suffix indicates a group of lncRNAs that  
9 are positioned on the opposite strand, with overlapping sequences to their juxtaposed protein-  
10 coding genes. Often, these lncRNAs play a role in regulating the expression of their protein-  
11 coding counterparts (22). Therefore, we set out to examine whether this is also the case for  
12 *RNF144A-AS1* (Figure 3B-C). Neither knockdown nor overexpression of *RNF144A-AS1*  
13 affected RNF144A transcript levels in MSCs cultured with or without TGF- $\beta$ 3. Moreover,  
14 RNF144A protein translation also remained unaffected with variations of *RNF144A-AS1* levels,  
15 as indicated by western blot (Figure 3D). These results indicate that *RNF144A-AS1* is not  
16 involved in the regulation of RNF144A. For these reasons, we proposed an alternative name for  
17 *RNF144A-AS1*: *GRASLND* - *Glycosaminoglycan Regulatory ASsociated Long Non-coDing*  
18 *RNA*.

19 Next, we explored the signaling axis of *GRASLND*. Data mining and computational analysis  
20 on earlier published data suggested that *GRASLND* was a downstream effector of SOX9  
21 (GSE69110) (37). When SOX9 was overexpressed in fibroblasts, *GRASLND* expression was  
22 increased (~ 2-fold). We further confirmed this by utilizing SOX9 transgene overexpression in  
23 our MSCs culture (Figure 3E). Interestingly, while TGF- $\beta$ 3 has been demonstrated to act  
24 upstream of SOX9, exogenous addition of this growth factor alone did not result in enhanced  
25 *GRASLND* expression. It is notable that SOX9 levels in GFP controls were indistinguishable  
26 between TGF- $\beta$ 3 conditions at the time of investigation (1 week in monolayer culture),

1 consistent with our previous finding that SOX9 was not upregulated until later timepoints in MSC  
2 chondrogenesis (36). Therefore, TGF- $\beta$ 3, despite being a potent growth factor, is not sufficient  
3 to elevate *GRASLND* expression. Instead, *GRASLND* appeared to be a downstream target of  
4 SOX9.

### 5 **Enhanced chondrogenesis for cartilage tissue engineering with *GRASLND***

6 As knockdown of *GRASLND* inhibited GAG and collagen deposition, we sought to  
7 investigate whether overexpression of *GRASLND* would enhance chondrogenesis. We  
8 assessed this question by both transgene ectopic expression and by CRISPR-dCas9 (Clustered  
9 regularly interspaced short palindromic repeats – catalytically dead Cas9) mediated in-locus  
10 activation.

11 We designed our lentiviral transfer vector to carry a BGH-pA (Bovine Growth Hormone  
12 Polyadenylation) termination signal downstream of *GRASLND* to allow for its correct processing  
13 (Figure S4A). Additionally, *GRASLND* was also driven under a doxycycline inducible promoter,  
14 enabling the temporal control of its expression. We utilized this feature to induce *GRASLND*  
15 only during chondrogenic culture (Figure 4A). This experimental design focused solely on the  
16 role of *GRASLND* during chondrogenesis, while successfully eliminating its effect in MSC  
17 maintenance and expansion from our analysis. As control, a vector encoding the *Discosoma* sp.  
18 red fluorescent protein (dsRed) coding sequence in place of *GRASLND* was utilized. Since  
19 doxycycline was most potent at 1  $\mu$ g/mL (Figure S4 B-C), this dose was used for all following  
20 experiments.

21 To determine whether *GRASLND* would improve chondrogenesis at lower doses of growth  
22 factor or at earlier time points, we compared DNA and GAG levels from pellets cultured under  
23 different TGF- $\beta$ 3 concentrations on day 7, day 14, and day 21 (Figure S4 D-F). In agreement  
24 with our knockdown data, DNA content was unaffected. On the other hand, increases in GAG  
25 were observed at higher doses and at later time points, especially at 10 ng/mL of TGF- $\beta$ 3. It  
26 appears that an elevated level of *GRASLND* alone was not sufficient to enhance GAG

1 deposition, and *GRASLND* may act in concert with other downstream effectors, which were not  
2 present at lower doses of TGF- $\beta$ 3 or at earlier time points in the process.

3 Elevated levels of *GRASLND* resulted in higher amounts of GAG deposition ( $p < 0.001$ )  
4 (Figure 4B), consistent with our data on the gene expression level (Figure 4D). We observed a  
5 slight increase in chondrogenic markers (*COL2A1*, *ACAN*), and a slight decrease in the  
6 apoptotic marker *CASP3*, while cellular senescence was not different between the two groups  
7 (*TP53*) (Figure 4D). Histologically, pellets derived from dsRed-transduced MSCs exhibited  
8 normal GAG and collagen type II staining, indicating successful chondrogenesis. The control  
9 pellets were indistinguishable from those derived from *GRASLND*-transduced MSCs (Figure  
10 4F), albeit macroscopically smaller at the time of harvest.

11 These findings were further confirmed using CRISPR-dCas9-VP64 mediated activation of  
12 endogenous *GRASLND*. This system had been previously utilized to upregulate various  
13 transcription factors that efficiently induce embryonic fibroblasts into neurons (43, 44). After  
14 screening eleven synthetic gRNAs, we selected the one with highest activation level (Figure  
15 S5). When *GRASLND* was transcriptionally activated with CRISPR-dCas9, chondrogenesis was  
16 enhanced as evidenced by elevated amount of GAG deposition ( $p < 0.01$ ); DNA amount may  
17 also be slightly increased, albeit not statistically significant (Figure 4C). Similar trends were  
18 detected by qRT-PCR (Figure 4E) and histology (Figure 4F). It is worth noting that CRISPR-  
19 dCas9 mediated activation only resulted in a moderate up-regulation of *GRASLND* relative to  
20 transgene ectopic expression (2-fold vs 100-fold). However, the functional outcome was more  
21 pronounced with CRISPR-dCas9. We observed approximately 50% increase in the level of  
22 GAG produced when normalized to DNA ( $9.4 \pm 2.19$  mg/mg vs  $16.3 \pm 2.08$  mg/mg), compared  
23 to 30% detected with ectopic expression ( $10.5 \pm 0.84$  mg/mg vs  $13.9 \pm 0.52$  mg/mg).



1 ***GRASLND* inhibits type II interferon signaling potentially by binding to EIF2AK2 and**  
2 **protects engineered cartilage from interferon**

3 To decipher the potential signaling pathways involved, we chondrogenically induced MSCs  
4 in the presence or absence of *GRASLND*, and then utilized RNA-seq to compare the global  
5 transcriptomic changes between two conditions. As expected, *GRASLND* depletion resulted in  
6 impaired expression of chondrocyte-associated genes such as *TRPV4* and *COL9A2* (top 20  
7 downregulated genes ranked by adjusted p-values) (Figure 5A). Skeletal system development  
8 and extracellular matrix organization were among the pathways most affected by the  
9 knockdown (Figure 5B). Surprisingly, pathways pertaining to interferon response were highly  
10 enriched in the upregulated gene list upon silencing of *GRASLND*. The top 20 upregulated  
11 genes involved many IFN downstream targets (*MX2*, *IFI44*, *IFI44L*, *IFITM1*, *IFI6*, *IFIT1*, *STAT1*,  
12 *MX1*, *IFIT3*, *OAS3*, *OAS2*), with both type I (IFN- $\alpha$ , IFN- $\beta$ ) and type II (IFN- $\gamma$ ) found to be  
13 enriched in our gene ontology analysis (Figure 5B). Furthermore, upregulated genes were also  
14 found to exhibit DNA binding motifs for transcription factors of the IFN pathways: *STAT1*,  
15 *STAT2*, *IRF1*, *IRF2* (Table 2). A full list of differentially expressed genes is provided in  
16 Supplementary Materials. Further bioinformatic analyses created a network of potential  
17 transcription regulators as well as gene ontology terms for the upregulated gene cohort as a  
18 result of *GRASLND* silencing (Figure 5C). Taken together, *GRASLND* may potentially act to  
19 suppress the activities of these transcription factors, as a result affecting IFN signaling pathways  
20 during chondrogenesis.

21 To further confirm this relationship, we performed luciferase reporter assays for interferon  
22 signaling upon *GRASLND* knockdown. Utilizing specific reporter constructs, we were able to  
23 determine whether *GRASLND* acted on type I or type II IFN. Our results indicated that  
24 decreased level of *GRASLND* led to heightened type II (IFN- $\gamma$ ) (Figure 5E) response but not  
25 type I (IFN- $\beta$ ) (Figure 5D). Importantly, luminescence activities between scrambled control and  
26 *GRASLND* knockdown were indistinguishable from each other in basal, IFN-free conditions.



1 This indicates that at basal level, the two groups responded similarly to lentiviral transduction,  
2 and the observed difference in IFN signal was a consequence of *GRASLND* downregulation.

3 Since *GRASLND* was expressed in the cytoplasm (Figure 2C), we hypothesized that it is  
4 part of an RNA-protein complex. To test this, we performed an RNA pull down assay, followed  
5 by mass spectrometry. Here, streptavidin beads were used as control, or conjugated to sense or  
6 antisense strands of *GRASLND*. Naked or conjugated beads were then incubated with lysates  
7 from day 21 pellets, from which bound proteins were eluted for further analyses. We found that  
8 Interferon-Induced Double-Stranded RNA-Activated Protein Kinase (EIF2AK2) peptides were  
9 detected at elevated levels in sense samples as compared to antisense controls ( $p < 0.05$ );  
10 peptides were undetected in naked bead controls. Subsequent RNA pull-down followed by  
11 western blot confirmed EIF2AK2 as a binding partner of *GRASLND* (Figure S6). We detected an  
12 increased level of EIF2AK2 bound to the sense strand of *GRASLND* relative to the antisense or  
13 the pellet lysate control. We speculate that this association of *GRASLND* RNA to EIF2AK2  
14 could potentially result in downregulation of IFN- $\gamma$  signaling.

15 Interestingly, by mining a published microarray database (GSE57218) (45), we found that  
16 IFN-related genes were highly elevated in cartilage tissues of osteoarthritis patients: *STAT1*,  
17 *IFNGR2*, *NCAM1*, *MID1* (Figure S7A). Since the microarray did not contain probes for  
18 *GRASLND*, no information on its expression could be extracted. In addition, we identified  
19 another independent study that reported changes in the transcriptomes of intact and damaged  
20 cartilage tissues (E-MTAB-4304) (46). Similarly, a cohort of IFN-related genes were also  
21 upregulated in damaged cartilage, especially *STAT1* and *IFNGR1* (Figure S7B). Interestingly,  
22 we identified a negative correlation between *GRASLND* and a few IFN related genes (*IFNGR1*,  
23 *ICAM1*) in damaged cartilage (Figure S7C). Therefore, we proposed that *GRASLND* may  
24 possess some therapeutic potential through suppressing IFN signaling in osteoarthritis. To  
25 evaluate this possibility, we implemented the use of the *GRASLND* transgene in engineered  
26 cartilage cultured under IFN addition (100 ng/mL of IFN- $\beta$  or 5 ng/mL of IFN- $\gamma$ ). We determined

1 doses of IFN- $\beta$  and IFN- $\gamma$  by selecting the lowest concentration at which day 21 pellets exhibited  
2 GAG loss compared to no IFN control. Consistent with luciferase reporter assays, the protective  
3 effect of *GRASLND* was observed upon IFN- $\gamma$  challenge but not IFN- $\beta$  (Figure 5F, G). However,  
4 we observed a reduced level of GAG production compared to normal conditions, suggesting  
5 that *GRASLND* can protect the ECM from degradation, but not completely to control levels.

### 6 ***GRASLND* enhanced the chondrogenesis of adipose-derived stem cells**

7 To determine if the function of *GRASLND* is unique to MSCs or present in other adult stem  
8 cells, we addressed whether modulating *GRASLND* expression could also improve  
9 chondrogenesis of adipose stem cells (ASCs). We observed an increase in GAG production  
10 when *GRASLND* was overexpressed in ASCs compared to control ( $p < 0.0001$ ) (Figure 6A),  
11 although *ACAN* levels were not significantly increased. Importantly, *COL2A1* expression was  
12 significantly elevated (~ 5-fold) with overexpression of *GRASLND* (Figure 6B). Histologic  
13 examination of the engineered cartilage showed a similar level of collagen type II in pellets with  
14 *GRASLND* overexpression compared to the dsRed control (Figure 6C). Based on these data, it  
15 appears that *GRASLND* utilized the same mechanism across these two cell types, asserting a  
16 pan effect on potentiating their chondrogenic capabilities.

17

### 18 ***Discussion***

19 Here, we identified and demonstrated the first functional study of lncRNA *GRASLND*, which  
20 acts to enhance stem cell chondrogenesis. Knockdown of *GRASLND* via shRNA inhibited  
21 chondrogenesis, whereas ectopic transgene or CRISPR-based overexpression of *GRASLND*  
22 enhanced chondrogenesis of MSCs and ASCs. Pathway analysis revealed a link between  
23 *GRASLND* and IFN- $\gamma$  signaling pathway in this process, which was confirmed by the  
24 identification of EIF2AK2 as its binding partner. Unfortunately, lack of a known murine homolog

1 makes it difficult to study *GRASLND* *in vivo*, and thus future studies may require *GRASLND*  
2 transgenic models in primate species.

3 In the context of the musculoskeletal system, IFN is mostly recognized for its role in bone  
4 development and homeostasis (23-27, 30), myogenesis (29, 47, 48), as well as its crosstalk with  
5 TGF- $\beta$  in wound healing (49). Notably, IFN- $\gamma$  has been suggested to inhibit collagen synthesis in  
6 dermal fibroblasts, myofibroblasts, and articular chondrocytes (49-53). Furthermore, the  
7 JAK/STAT pathway, which involves IFN downstream effectors, has also been shown to inhibit  
8 chondrocyte proliferation and differentiation (28, 31). Here, we found that *GRASLND* acts to  
9 suppress the IFN mechanism. In addition, we also present evidence indicating an interaction  
10 between *GRASLND* and EIF2AK2 (also referred to as PKR). Canonically a crucial player in  
11 protein synthesis, PKR has also been reported to control STAT signaling by directly binding to  
12 and preventing its association with DNA for gene activation (54, 55). Additionally, several  
13 studies have suggested that highly structured, single stranded RNA can also activate PKR via  
14 its double stranded RNA binding domains (dsDRBs) (56-60). Our RNA-seq data suggested that  
15 upon *GRASLND* knockdown, a cohort of downstream targets of STATs were upregulated.  
16 Based on the presence of DNA binding motifs in investigated targets, we identified both STAT1  
17 and STAT2 as potential regulators of genes disrupted by *GRASLND* knockdown. However, our  
18 luciferase reporter assays pointed towards a mechanism in IFN type II (gene activation by  
19 STAT1 homodimer) rather than type I (gene activation by STAT1/STAT2 heterodimer). Thus,  
20 we hypothesized that *GRASLND* could form a secondary structure to bind and activate PKR,  
21 which in turn inhibits STAT1-related transcriptional function. This mechanism supports the  
22 hypothesis that modulation of IFN- $\gamma$  via the JAK/STAT pathway, achieved by the  
23 *GRASLND*/PKR RNA-protein complex, is important for cellular proliferation and differentiation  
24 during chondrogenesis.

25 Upregulation of IFN has also been implicated in arthritis by several studies (61-64). Publicly  
26 available databases provide evidence corroborating similar patterns of IFN in degenerated

1 cartilage. As *GRASLND* inhibits IFN, utilization of this lncRNA offers potential in both MSC  
2 cartilage tissue engineering and in OA treatment. As a proof of concept, we showed that  
3 *GRASLND* could enhance matrix deposition across cell types of origin, with and without  
4 interferon challenge *in vitro*. It would be interesting to next investigate whether *GRASLND* can  
5 protect cartilage from degradation in a milieu of pro-inflammatory cytokines *in vivo*.

6 Since lentivirus was employed to manipulate the expression of *GRASLND*, it is possible our  
7 observations were confounded by the cellular response to viral infection. However, our  
8 luciferase reporter assays demonstrated that basal luminescence levels (with no interferon  
9 supplementation) between the scrambled controls and the shRNA treatments were  
10 indistinguishable. This suggests that altered levels of interferon signaling can be attributed to  
11 experimentally varied levels of *GRASLND* and not to the presence of lentivirus. Our data  
12 indicate that *GRASLND* acts through type II rather than type I IFN. We found that 5 ng/mL of  
13 IFN- $\gamma$  was still more detrimental to chondrogenic constructs compared to 100 ng/mL of IFN- $\beta$ .  
14 One potential explanation for this phenomenon may be the skewed distribution of available  
15 surface receptors between type I and type II (IFNAR vs IFNGR). Indeed, MSCs express a much  
16 lower level of *IFNAR2* compared to *IFNAR1*, *IFNGR1*, or *IFNGR2* (both in GSE109503 (36) and  
17 in GSE129985 (this manuscript)). As these receptors function as heterodimers (32, 34),  
18 response to type I may be stunted due to *IFNAR2* deficiency.

19 Furthermore, we showed that a modified CRISPR-dCas9 system could successfully be used  
20 for endogenous transcriptional activation of lncRNA. This system had been previously used in  
21 other cell types to regulate expression of both protein-coding and non-coding genes (43, 44, 65,  
22 66). We showed that CRISPR may be more effective than transgene expression, as indicated  
23 by a larger increase in GAG production, despite lower levels of overall gene activation. As  
24 *GRASLND* does not regulate *RNF144A*, it is evident that *GRASLND* acts *in trans*. However, we  
25 speculate the CRISPR-dCas9 system could also be useful for gain of function studies to

1 investigate lncRNAs acting *in cis*, as well as lncRNAs that are difficult to obtain via molecular  
2 cloning due to their secondary structures, high repeated sequence or GC-rich content.

3 In conclusion, we have identified *GRASLND* as an important regulator of chondrogenesis.  
4 *GRASLND* acts downstream of SOX9 and enhances cartilage-like matrix deposition in stem  
5 cell-derived constructs. Moreover, *GRASLND* functions to suppress IFN via PKR, and as a  
6 result induces adult stem cells towards a more chondrocyte-like lineage. It is likely that the  
7 *GRASLND*/PKR RNA-protein complex may inhibit STAT1 transcriptional activity. We propose  
8 that *GRASLND* can potentially be applied therapeutically for both cartilage tissue engineering  
9 and for the treatment of OA.

10

## 11 **Materials and Methods**

### 12 **Cell culture**

13 Bone marrow was obtained from discarded and de-identified waste tissue from adult bone  
14 marrow transplant donors in accordance with the Institutional Review Board of Duke University  
15 Medical Center. Adherent cells were expanded and maintained in expansion medium: DMEM-  
16 low glucose (Gibco), 1% Penicillin/streptomycin (Gibco), 10% fetal bovine serum (FBS)  
17 (ThermoFisher), and 1 ng/mL basic fibroblast growth factor (Roche) (67).

18 Adipose derived stem cells (ASCs) were purchased from ATCC (SCRC-4000) and cultured  
19 in complete growth medium: Mesenchymal stem cells basal medium (ATCC PCS-500-030),  
20 mesenchymal stem cell growth kit (ATCC PCS-500-040) (2% FBS, 5 ng/mL basic recombinant  
21 human FGF, 5 ng/mL acidic recombinant human FGF, 5 ng/mL recombinant human EGF, 2.4  
22 nM L-alanyl-L-glutamine), 0.2 mg/mL G418.

### 23 **Plasmid construction**

#### 24 shRNA

25 Short hairpin RNA (shRNA) sequences for specific genes of interest were designed with the  
26 Broad Institute GPP Web Portal (68). For each gene, six different sequences were selected for

1 screening, after which the two most effective were chosen for downstream experiments in  
2 chondrogenic assays. Selected shRNAs were cloned into a modified lentiviral vector (Addgene  
3 #12247) using MluI and ClaI restriction sites, as described previously (69). A complete list of  
4 effective shRNA sequences is presented in Table S1.

#### 5 **Transgene overexpression of *GRASLND***

6 A derivative vector from modified TMPrtTA (3, 70) was created with NEBuilder® HiFi DNA  
7 Assembly Master Mix (New England Biolabs). Backbone was digested with EcoRV-HF (New  
8 England Biolabs) and PspXI (New England Biolabs). The following resultant fragments were  
9 amplified by polymerase chain reaction and assembled into the digested plasmid: Tetracycline  
10 responsive element and minimal CMV promoter (TRE/CMV), Firefly luciferase, bGH poly(A)  
11 termination signal (BGHpA). Primers and plasmids for cloning are provided in Table S2.

12 The full sequence of *GRASLND* transcript variant 1 (RefSeq NR\_033997.1) was  
13 synthesized by Integrated DNA Technologies, Inc. *GRASLND* or the *Discosoma* sp. red  
14 fluorescent protein coding sequence (dsRed) were cloned into the above derivative tetracycline  
15 inducible plasmid with NEBuilder® HiFi DNA Assembly Master Mix (New England Biolabs) at  
16 NheI and MluI restriction sites (pLVD-*GRASLND* and pLVD-dsRed). Amplifying primers are  
17 provided in Table S2.

#### 18 **CRISPR-dCas9 activation of *GRASLND***

19 Guide RNA sequences were designed using the UCSC genome browser  
20 (<http://genome.ucsc.edu/>) (71), integrated with the MIT specificity score calculated by CRISPOR  
21 and the Doench efficiency score (72, 73). Oligonucleotides (IDT, Inc) were phosphorylated,  
22 annealed, and ligated into the pLV-hUbc-dCas9-VP64 lentiviral transfer vector (Addgene  
23 #53192) previously digested at BsmBI restriction sites (74). Eleven potential guide RNA  
24 sequences were selected and screened for their efficacy, and the gRNA with the highest  
25 activation potential was chosen for further experiments (Figure S5). The synthetic gRNA used in

1 all CRISPR-dCas9 activation experiments has the following sequence: 5'-

2 CCACTGGGGATAGTTCCTG-3'.

### 3 **Chondrogenesis assay**

4 MSCs or ASCs were digested in 0.05% Trypsin-EDTA (Gibco), and trypsin was inactivated  
5 with 1.5X volume of expansion medium. Dissociated cells were centrifuged at 200 x g for 5  
6 minutes, and supernatant was aspirated. Subsequently, cells were washed in pre-warmed  
7 DMEM-high glucose (Gibco) three times, and resuspended at  $5 \times 10^5$  cells/mL in complete  
8 chondrogenic medium: DMEM-high glucose (Gibco), 1% Penicillin/ streptomycin (Gibco), 1%  
9 ITS+ (Corning), 100 nM Dexamethasone (Sigma-Aldrich), 50  $\mu$ g/mL ascorbic acid (Sigma-  
10 Aldrich), 40  $\mu$ g/mL L-proline (Sigma-Aldrich), 10 ng/mL rhTGF- $\beta$ 3 (R&D Systems). Five hundred  
11  $\mu$ L of the above cell mixture was dispensed into 15 mL conical tubes, and centrifuged at 200 x g  
12 for 5 minutes. Pellets were cultured at 37°C, 5% CO<sub>2</sub> for 21 days with medium exchange every  
13 three days.

### 14 **Osteogenesis and adipogenesis assays**

15 MSCs were plated at  $2 \times 10^4$  cells/well in 6-well plates (Corning) and cultured for 4 days in  
16 MSC expansion medium, followed by induction medium for 7 days. Osteogenic induction  
17 medium includes: DMEM-high glucose (Gibco), 10% FBS, 1% Penicillin/ streptomycin (Gibco),  
18 10 nM Dexamethasone (Sigma-Aldrich), 50  $\mu$ g/mL ascorbic acid (Sigma-Aldrich), 40  $\mu$ g/mL L-  
19 proline (Sigma-Aldrich), 10 mM  $\beta$ -glycerol phosphate (Chem-Impex International), 100 ng/mL  
20 rh-BMP2 (ThermoFisher). Adipogenic induction medium includes: DMEM-high glucose (Gibco),  
21 10% FBS (ThermoFisher), 1% Penicillin/ streptomycin (Gibco), 1% ITS+ (Corning), 100 nM  
22 Dexamethasone (Sigma-Aldrich), 450  $\mu$ M 3-isobutyl-1-methylxanthine (Sigma-Aldrich), 200  $\mu$ M  
23 indomethacin (Sigma-Aldrich).

### 24 **Biochemical assays**

25 Harvested pellets were stored at -20°C until further processing. Collected samples were  
26 digested in 125  $\mu$ g/mL papain at 60°C overnight. DMMB assay was performed as previously

1 described to measure GAG production (76). PicoGreen assay (ThermoFisher) was performed to  
2 measure DNA content following manufacture's protocol.

### 3 **Immunohistochemistry and histology**

4 Harvested pellets were fixed in 4% paraformaldehyde for 48 hours, and processed for  
5 paraffin embedding. Samples were sectioned at 10 µm thickness, and subjected to either  
6 Safranin O – Fast Green standard staining (77) or to immunohistochemistry of collagen type II  
7 (Developmental Studies Hybridoma Bank, University of Iowa; #II-II6B3). Human osteochondral  
8 sections were stained simultaneously to serve as positive control. Sections with no primary  
9 antibodies were used as negative control for immunohistochemistry.

### 10 **RNA fluorescence in situ hybridization (RNA FISH)**

11 Harvested pellets were snap frozen in Tissue-Plus O.C.T. Compound (Fisher HealthCare)  
12 and stored at -80°C until further processing. Samples were sectioned at 5 µm thickness and  
13 slides were stored at -80°C until staining. Probe sets for RNA FISH were conjugated with  
14 Quasar® 670 dye, and were synthesized by LGC Biosearch Technologies and listed in Table  
15 S3 (*RNF144A-AS1*). GAPDH probe set was pre-designed by the manufacturer. Staining was  
16 carried out according to manufacturer's protocol for frozen tissues. Slides were mounted with  
17 Prolong Gold anti-fade mountant with DAPI (ThermoFisher) and imaged with the Virtual Slide  
18 Microscope VS120 (Olympus) at lower magnification and with the confocal microscope (Zeiss)  
19 at higher magnification.

### 20 **RNA isolation and quantitative RT-PCR**

21 Norgen Total RNA Isolation Plus Micro Kits (Norgen Biotek) were used to extract RNA from  
22 pellet samples and Norgen Total RNA Isolation Plus Kits (Norgen Biotek) were used for all other  
23 RNA isolation. For monolayer, cells were lysed in buffer RL and stored at -20°C until further  
24 processing. For pellets, harvested samples were snap frozen in liquid nitrogen and stored at -  
25 80°C until further processing. On day of RNA isolation, pellets were homogenized in buffer RL



1 using a bead beater (BioSpec Products) at 2,500 oscillations per minute for 20 seconds for a  
2 total of three times. Subsequent steps were performed following manufacturer's protocol.

3 Nuclear and cytoplasmic fractions from day 21 MSC pellets were separated with the NE-  
4 PER Nuclear and Cytoplasmic Extraction Reagents (ThermoFisher) following manufacturer's  
5 protocol. Resulting extracts were immediately subjected to RNA isolation using the Norgen Total  
6 RNA Isolation Plus Micro Kits (Norgen Biotek) by adding 2.5 parts of buffer RL to 1 part of  
7 extract. Subsequent steps were carried out following manufacturer's protocol.

8 Reverse transcription by Superscript VILO cDNA master mix (Invitrogen) was performed  
9 immediately following RNA isolation. cDNA was stored at -20°C until further processing. qRT-  
10 PCR was carried out using Fast SyBR Green master mix (Applied Biosystems) following  
11 manufacturer's protocol. A complete list of primer pairs (synthesized by Integrated DNA  
12 Technologies, Inc.) is reported in Table S4.

### 13 **Luminescence assay**

14 MSCs were plated at  $8.5 \times 10^4$  cells per well in 24-well plates (Corning). Lentivirus carrying  
15 the response elements for type I (ISRE - #CLS-008L-1) or type II (GAS - #CLS-009L-1)  
16 upstream of firefly luciferase was purchased from Qiagen. Twenty-four hours post plating, cells  
17 were co-transduced with virus in the following groups: ISRE with scrambled shRNA, ISRE with  
18 *GRASLND* shRNA, GAS with scrambled shRNA, GAS with *GRASLND* shRNA. Twenty-four  
19 hours post-transduction, cells were rinsed once in PBS and fresh medium was exchanged.  
20 Three days later, medium was switched to expansion medium with 100 ng/mL IFN- $\beta$   
21 (PeproTech) for wells with ISRE or with 5 ng/mL IFN- $\gamma$  (PeproTech) for wells with GAS. MSCs  
22 were cultured for another 22 hours, and then harvested for luminescence assay using Bright-  
23 Glo Luciferase Assay System (Promega). Luminescence signals were measured using the  
24 Cytation 5 Plate reader (BioTek).

## 1 **Western blot**

2 On day of harvest, cells were homogenized with complete lysis buffer in ice cold PBS: 10X  
3 RIPA buffer (Cell Signaling Technology), 100X phosphatase inhibitor cocktail A (Santa Cruz  
4 Biotechnology), 100X Halt™ protease inhibitor cocktails (ThermoScientific). Lysates were  
5 subsequently centrifuged at 14,000 x g for 15 minutes at 4°C, and supernatants were collected  
6 and stored at -20°C until further processing. Western blot was serviced by RayBiotech with the  
7 following antibodies: primary anti-β-actin (RayBiotech), primary anti-RNF144A (Abcam), primary  
8 anti-PKR (RayBiotech) and secondary anti-rabbit-HRP (horse radish peroxidase) (RayBiotech).

## 9 **Statistical analyses**

10 All statistical analyses were performed using R (78). Results from biochemical assays are  
11 depicted as mean ± SD. Results from qRT-PCR are depicted as fold-change with error bars  
12 calculated per Applied Biosystems manual instruction.

13 Additional methods are provided in supplemental information.

## 14 **Acknowledgments**

15 We thank the Genome Technology Access Center at Washington University in St Louis, the  
16 Proteomics Core Laboratory, and the Hope Center Viral Vectors Core for their resources and  
17 support. The CRISPR-dCas9-VP64 system was a generous gift from Dr. Charles Gersbach. We  
18 also wish to thank Sara Oswald for providing assistance in technical writing of the manuscript.

19 This work was supported by the Arthritis Foundation, NIH grants AR50245, AR48852,  
20 AG15768, AR48182, AR067467, AR057235, AR073752, the Nancy Taylor Foundation for  
21 Chronic Diseases, and the Collaborative Research Center of the AO Foundation, Davos,  
22 Switzerland.

23 **Author contributions:** N.P.T.H, F.G designed research; N.P.T.H., C.C.G., J.L. and R.T.  
24 performed research and analyzed data; J.M.B., A.M., and B.Z. provided critical discussion and  
25 comments. N.P.T.H. and F.G. wrote the manuscript; all authors edited the manuscript.

26 **Accession number:** GSE129985

## 1 **References**

- 2 1. Sophia Fox AJ, Bedi A, & Rodeo SA (2009) The basic science of articular cartilage:  
3 structure, composition, and function. *Sports Health* 1(6):461-468.
- 4 2. Huynh NPT, *et al.* (2018) Genetic Engineering of Mesenchymal Stem Cells for  
5 Differential Matrix Deposition on 3D Woven Scaffolds. *Tissue Eng Part A* 24(19-  
6 20):1531-1544.
- 7 3. Glass KA, *et al.* (2014) Tissue-engineered cartilage with inducible and tunable  
8 immunomodulatory properties. *Biomaterials* 35(22):5921-5931.
- 9 4. Brunger JM, Zutshi A, Willard VP, Gersbach CA, & Guilak F (2017) CRISPR/Cas9  
10 Editing of Murine Induced Pluripotent Stem Cells for Engineering Inflammation-Resistant  
11 Tissues. *Arthritis Rheumatol* 69(5):1111-1121.
- 12 5. Brunger JM, Zutshi A, Willard VP, Gersbach CA, & Guilak F (2017) Genome  
13 Engineering of Stem Cells for Autonomously Regulated, Closed-Loop Delivery of  
14 Biologic Drugs. *Stem Cell Reports* 8(5):1202-1213.
- 15 6. Brunger JM, *et al.* (2014) Scaffold-mediated lentiviral transduction for functional tissue  
16 engineering of cartilage. *Proc Natl Acad Sci U S A* 111(9):E798-806.
- 17 7. Adkar SS, *et al.* (2017) Genome Engineering for Personalized Arthritis Therapeutics.  
18 *Trends Mol Med* 23(10):917-931.
- 19 8. Gimble J & Guilak F (2003) Adipose-derived adult stem cells: isolation, characterization,  
20 and differentiation potential. *Cytotherapy* 5(5):362-369.
- 21 9. Erickson GR, *et al.* (2002) Chondrogenic potential of adipose tissue-derived stromal  
22 cells in vitro and in vivo. *Biochem Biophys Res Commun* 290(2):763-769.
- 23 10. Awad HA, Wickham MQ, Leddy HA, Gimble JM, & Guilak F (2004) Chondrogenic  
24 differentiation of adipose-derived adult stem cells in agarose, alginate, and gelatin  
25 scaffolds. *Biomaterials* 25(16):3211-3222.
- 26 11. Caplan AI (1991) Mesenchymal stem cells. *J Orthop Res* 9(5):641-650.
- 27 12. Mackay AM, *et al.* (1998) Chondrogenic differentiation of cultured human mesenchymal  
28 stem cells from marrow. *Tissue Eng* 4(4):415-428.
- 29 13. Johnstone B, Hering TM, Caplan AI, Goldberg VM, & Yoo JU (1998) In vitro  
30 chondrogenesis of bone marrow-derived mesenchymal progenitor cells. *Exp Cell Res*  
31 238(1):265-272.
- 32 14. Lander ES, *et al.* (2001) Initial sequencing and analysis of the human genome. *Nature*  
33 409(6822):860-921.
- 34 15. Guttman M, *et al.* (2009) Chromatin signature reveals over a thousand highly conserved  
35 large non-coding RNAs in mammals. *Nature* 458(7235):223-227.
- 36 16. Guttman M, *et al.* (2011) lincRNAs act in the circuitry controlling pluripotency and  
37 differentiation. *Nature* 477(7364):295-300.
- 38 17. Lee JT & Bartolomei MS (2013) X-inactivation, imprinting, and long noncoding RNAs in  
39 health and disease. *Cell* 152(6):1308-1323.
- 40 18. Ng SY, Johnson R, & Stanton LW (2012) Human long non-coding RNAs promote  
41 pluripotency and neuronal differentiation by association with chromatin modifiers and  
42 transcription factors. *EMBO J* 31(3):522-533.
- 43 19. Briggs JA, Wolvetang EJ, Mattick JS, Rinn JL, & Barry G (2015) Mechanisms of Long  
44 Non-coding RNAs in Mammalian Nervous System Development, Plasticity, Disease, and  
45 Evolution. *Neuron* 88(5):861-877.
- 46 20. Carlson HL, *et al.* (2015) LncRNA-HIT Functions as an Epigenetic Regulator of  
47 Chondrogenesis through Its Recruitment of p100/CBP Complexes. *PLoS Genet*  
48 11(12):e1005680.

- 1 21. Barter MJ, *et al.* (2017) The long non-coding RNA ROCR contributes to SOX9  
2 expression and chondrogenic differentiation of human mesenchymal stem cells.  
3 *Development* 144(24):4510-4521.
- 4 22. Huynh NP, Anderson BA, Guilak F, & McAlinden A (2017) Emerging roles for long  
5 noncoding RNAs in skeletal biology and disease. *Connect Tissue Res* 58(1):116-141.
- 6 23. Dieudonne FX, *et al.* (2013) Promotion of osteoblast differentiation in mesenchymal cells  
7 through Cbl-mediated control of STAT5 activity. *Stem Cells* 31(7):1340-1349.
- 8 24. Rostovskaya M, *et al.* (2018) Clonal Analysis Delineates Transcriptional Programs of  
9 Osteogenic and Adipogenic Lineages of Adult Mouse Skeletal Progenitors. *Stem Cell*  
10 *Reports* 11(1):212-227.
- 11 25. Takayanagi H, *et al.* (2002) RANKL maintains bone homeostasis through c-Fos-  
12 dependent induction of interferon-beta. *Nature* 416(6882):744-749.
- 13 26. Takayanagi H, Kim S, & Taniguchi T (2002) Signaling crosstalk between RANKL and  
14 interferons in osteoclast differentiation. *Arthritis Res* 4 Suppl 3:S227-232.
- 15 27. Li J (2013) JAK-STAT and bone metabolism. *JAKSTAT* 2(3):e23930.
- 16 28. Sahni M, *et al.* (1999) FGF signaling inhibits chondrocyte proliferation and regulates  
17 bone development through the STAT-1 pathway. *Genes Dev* 13(11):1361-1366.
- 18 29. Jang YN & Baik EJ (2013) JAK-STAT pathway and myogenic differentiation. *JAKSTAT*  
19 2(2):e23282.
- 20 30. Xiao L, *et al.* (2004) Stat1 controls postnatal bone formation by regulating fibroblast  
21 growth factor signaling in osteoblasts. *J Biol Chem* 279(26):27743-27752.
- 22 31. Sahni M, Raz R, Coffin JD, Levy D, & Basilico C (2001) STAT1 mediates the increased  
23 apoptosis and reduced chondrocyte proliferation in mice overexpressing FGF2.  
24 *Development* 128(11):2119-2129.
- 25 32. Brierley MM & Fish EN (2002) Review: IFN-alpha/beta receptor interactions to biologic  
26 outcomes: understanding the circuitry. *J Interferon Cytokine Res* 22(8):835-845.
- 27 33. Hertzog PJ, Hwang SY, & Kola I (1994) Role of interferons in the regulation of cell  
28 proliferation, differentiation, and development. *Mol Reprod Dev* 39(2):226-232.
- 29 34. Hu X & Ivashkiv LB (2009) Cross-regulation of signaling pathways by interferon-gamma:  
30 implications for immune responses and autoimmune diseases. *Immunity* 31(4):539-550.
- 31 35. Green DS, Young HA, & Valencia JC (2017) Current prospects of type II interferon  
32 gamma signaling and autoimmunity. *J Biol Chem* 292(34):13925-13933.
- 33 36. Huynh NPT, Zhang B, & Guilak F (2018) High-depth transcriptomic profiling reveals the  
34 temporal gene signature of human mesenchymal stem cells during chondrogenesis.  
35 *FASEB J*:fj201800534R.
- 36 37. Ohba S, He X, Hojo H, & McMahon AP (2015) Distinct Transcriptional Programs  
37 Underlie Sox9 Regulation of the Mammalian Chondrocyte. *Cell Rep* 12(2):229-243.
- 38 38. Clemson CM, *et al.* (2009) An architectural role for a nuclear noncoding RNA: NEAT1  
39 RNA is essential for the structure of paraspeckles. *Mol Cell* 33(6):717-726.
- 40 39. Sasaki YT, Ideue T, Sano M, Mituyama T, & Hirose T (2009) MENepsilon/beta  
41 noncoding RNAs are essential for structural integrity of nuclear paraspeckles. *Proc Natl*  
42 *Acad Sci U S A* 106(8):2525-2530.
- 43 40. Rhesus Macaque Genome S, *et al.* (2007) Evolutionary and biomedical insights from the  
44 rhesus macaque genome. *Science* 316(5822):222-234.
- 45 41. Derrien T, *et al.* (2012) The GENCODE v7 catalog of human long noncoding RNAs:  
46 analysis of their gene structure, evolution, and expression. *Genome Res* 22(9):1775-  
47 1789.
- 48 42. Necsulea A, *et al.* (2014) The evolution of lncRNA repertoires and expression patterns in  
49 tetrapods. *Nature* 505(7485):635-640.

- 1 43. Black JB, *et al.* (2016) Targeted Epigenetic Remodeling of Endogenous Loci by  
2 CRISPR/Cas9-Based Transcriptional Activators Directly Converts Fibroblasts to  
3 Neuronal Cells. *Cell Stem Cell* 19(3):406-414.
- 4 44. Perez-Pinera P, *et al.* (2013) RNA-guided gene activation by CRISPR-Cas9-based  
5 transcription factors. *Nat Methods* 10(10):973-976.
- 6 45. Ramos YF, *et al.* (2014) Genes involved in the osteoarthritis process identified through  
7 genome wide expression analysis in articular cartilage; the RAAK study. *PLoS One*  
8 9(7):e103056.
- 9 46. Dunn SL, *et al.* (2016) Gene expression changes in damaged osteoarthritic cartilage  
10 identify a signature of non-chondrogenic and mechanical responses. *Osteoarthritis*  
11 *Cartilage* 24(8):1431-1440.
- 12 47. Cheng M, Nguyen MH, Fantuzzi G, & Koh TJ (2008) Endogenous interferon-gamma is  
13 required for efficient skeletal muscle regeneration. *Am J Physiol Cell Physiol*  
14 294(5):C1183-1191.
- 15 48. Londhe P & Davie JK (2011) Gamma interferon modulates myogenesis through the  
16 major histocompatibility complex class II transactivator, CIITA. *Mol Cell Biol*  
17 31(14):2854-2866.
- 18 49. Ishida Y, Kondo T, Takayasu T, Iwakura Y, & Mukaida N (2004) The essential  
19 involvement of cross-talk between IFN-gamma and TGF-beta in the skin wound-healing  
20 process. *J Immunol* 172(3):1848-1855.
- 21 50. Yufit T, Vining V, Wang L, Brown RR, & Varga J (1995) Inhibition of type I collagen  
22 mRNA expression independent of tryptophan depletion in interferon-gamma-treated  
23 human dermal fibroblasts. *J Invest Dermatol* 105(3):388-393.
- 24 51. Harrop AR, *et al.* (1995) Regulation of collagen synthesis and mRNA expression in  
25 normal and hypertrophic scar fibroblasts in vitro by interferon-gamma. *J Surg Res*  
26 58(5):471-477.
- 27 52. Granstein RD, Flotte TJ, & Amento EP (1990) Interferons and collagen production. *J*  
28 *Invest Dermatol* 95(6 Suppl):75S-80S.
- 29 53. Amento EP, Bhan AK, McCullagh KG, & Krane SM (1985) Influences of gamma  
30 interferon on synovial fibroblast-like cells. Ia induction and inhibition of collagen  
31 synthesis. *J Clin Invest* 76(2):837-848.
- 32 54. Wang S, *et al.* (2006) The catalytic activity of the eukaryotic initiation factor-2alpha  
33 kinase PKR is required to negatively regulate Stat1 and Stat3 via activation of the T-cell  
34 protein-tyrosine phosphatase. *J Biol Chem* 281(14):9439-9449.
- 35 55. Wong AH, *et al.* (1997) Physical association between STAT1 and the interferon-  
36 inducible protein kinase PKR and implications for interferon and double-stranded RNA  
37 signaling pathways. *EMBO J* 16(6):1291-1304.
- 38 56. Osman F, Jarrous N, Ben-Asouli Y, & Kaempfer R (1999) A cis-acting element in the 3'-  
39 untranslated region of human TNF-alpha mRNA renders splicing dependent on the  
40 activation of protein kinase PKR. *Genes Dev* 13(24):3280-3293.
- 41 57. Ben-Asouli Y, Banai Y, Pei-Or Y, Shir A, & Kaempfer R (2002) Human interferon-gamma  
42 mRNA autoregulates its translation through a pseudoknot that activates the interferon-  
43 inducible protein kinase PKR. *Cell* 108(2):221-232.
- 44 58. Cohen-Chalamish S, *et al.* (2009) Dynamic refolding of IFN-gamma mRNA enables it to  
45 function as PKR activator and translation template. *Nat Chem Biol* 5(12):896-903.
- 46 59. Nallagatla SR, *et al.* (2007) 5'-triphosphate-dependent activation of PKR by RNAs with  
47 short stem-loops. *Science* 318(5855):1455-1458.
- 48 60. Mayo CB & Cole JL (2017) Interaction of PKR with single-stranded RNA. *Sci Rep*  
49 7(1):3335.
- 50 61. Boissier MC, *et al.* (1995) Biphasic effect of interferon-gamma in murine collagen-  
51 induced arthritis. *Eur J Immunol* 25(5):1184-1190.



- 1 62. Cooper SM, Sriram S, & Ranges GE (1988) Suppression of murine collagen-induced  
2 arthritis with monoclonal anti-Ia antibodies and augmentation with IFN-gamma. *J*  
3 *Immunol* 141(6):1958-1962.
- 4 63. Westacott CI, *et al.* (1990) Synovial fluid concentration of five different cytokines in  
5 rheumatic diseases. *Ann Rheum Dis* 49(9):676-681.
- 6 64. Kahle P, *et al.* (1992) Determination of cytokines in synovial fluids: correlation with  
7 diagnosis and histomorphological characteristics of synovial tissue. *Ann Rheum Dis*  
8 51(6):731-734.
- 9 65. Bester AC, *et al.* (2018) An Integrated Genome-wide CRISPRa Approach to  
10 Functionalize lncRNAs in Drug Resistance. *Cell* 173(3):649-664 e620.
- 11 66. Liu SJ, *et al.* (2017) CRISPRi-based genome-scale identification of functional long  
12 noncoding RNA loci in human cells. *Science* 355(6320).
- 13 67. Hagmann S, *et al.* (2013) FGF-2 addition during expansion of human bone marrow-  
14 derived stromal cells alters MSC surface marker distribution and chondrogenic  
15 differentiation potential. *Cell Prolif* 46(4):396-407.
- 16 68. Moffat J, *et al.* (2006) A lentiviral RNAi library for human and mouse genes applied to an  
17 arrayed viral high-content screen. *Cell* 124(6):1283-1298.
- 18 69. Diekmann BO, *et al.* (2015) Knockdown of the cell cycle inhibitor p21 enhances cartilage  
19 formation by induced pluripotent stem cells. *Tissue Eng Part A* 21(7-8):1261-1274.
- 20 70. Barde I, *et al.* (2006) Efficient control of gene expression in the hematopoietic system  
21 using a single Tet-on inducible lentiviral vector. *Mol Ther* 13(2):382-390.
- 22 71. Kent WJ, *et al.* (2002) The human genome browser at UCSC. *Genome Res* 12(6):996-  
23 1006.
- 24 72. Doench JG, *et al.* (2016) Optimized sgRNA design to maximize activity and minimize off-  
25 target effects of CRISPR-Cas9. *Nat Biotechnol* 34(2):184-191.
- 26 73. Haeussler M, *et al.* (2016) Evaluation of off-target and on-target scoring algorithms and  
27 integration into the guide RNA selection tool CRISPOR. *Genome Biol* 17(1):148.
- 28 74. Kabadi AM, Ousterout DG, Hilton IB, & Gersbach CA (2014) Multiplex CRISPR/Cas9-  
29 based genome engineering from a single lentiviral vector. *Nucleic Acids Res*  
30 42(19):e147.
- 31 75. Sastry L, Johnson T, Hobson MJ, Smucker B, & Cornetta K (2002) Titering lentiviral  
32 vectors: comparison of DNA, RNA and marker expression methods. *Gene Ther*  
33 9(17):1155-1162.
- 34 76. Farndale RW, Buttle DJ, & Barrett AJ (1986) Improved quantitation and discrimination of  
35 sulphated glycosaminoglycans by use of dimethylmethylene blue. *Biochim Biophys Acta*  
36 883(2):173-177.
- 37 77. Estes BT, Diekmann BO, Gimble JM, & Guilak F (2010) Isolation of adipose-derived stem  
38 cells and their induction to a chondrogenic phenotype. *Nat Protoc* 5(7):1294-1311.
- 39 78. Team RC (2018) R: A language and environment for statistical computing. *R Foundation*  
40 *for Statistical Computing Vienna, Austria.*
- 41 79. Weirauch MT, *et al.* (2014) Determination and inference of eukaryotic transcription factor  
42 sequence specificity. *Cell* 158(6):1431-1443.
- 43

## 1 **Figure legends**

**Figure 1:** *RNF144A-AS1* is important and specifically upregulated in MSC chondrogenesis.

(A) Expression pattern of *RNF144A-AS1* in chondrogenesis (GSE109503 (36)). Log2TPM: log transformed value of transcripts per million (TPM). (B) Effect of *RNF144A-AS1* knockdown on chondrogenic, apoptotic, and cell cycle inhibition markers (n = 5). (C-E) Effect of *RNF144A-AS1* knockdown on pellet matrix synthesis (n = 5). (F) Representative histological images of day 21 MSC pellets. Scale bar = 200  $\mu$ m. *SafO-FG*: SafraninO-Fast Green staining. *COLII IHC*: collagen type II immunohistochemistry. *hOC*: human osteochondral control. (G-I) qRT-PCR analysis of MSC samples cultured in (G) adipogenic condition (n=6), (H) osteogenic condition (n=6), (I) chondrogenic condition (n=3-4). One-way ANOVA followed by Tukey post-hoc test ( $\alpha=0.05$ ). Groups of different letters are statistically different from one another.

**Figure 2:** *RNF144A-AS1* is localized to the cytoplasm.

(A) RNA in situ hybridization of MSC-derived pellets at different time points during chondrogenesis. *GAPDH* and *RNF144A-AS1* probes were hybridized on separate slides. Scale bar = 20  $\mu$ m. (B) qRT-PCR of nuclear versus cytoplasmic fraction of day 21 MSC pellets (n=4). (C) Confocal microscopy on MSC-derived pellets. Scale bar = 5  $\mu$ m. One-way ANOVA followed by Tukey post-hoc test ( $\alpha=0.05$ ). Groups of different letters are statistically different from one another.

**Figure 3:** *RNF144-AS1* relationship to *RNF144A* and *SOX9*.

(A) *RNF144A-AS1* genomic location and conservation across different species. Data retrieved from UCSC Genome Browser. (B) Knockdown of *RNF144A-AS1* and expression of *RNF144A* (n=4). (C) Overexpression *RNF144A-AS1* and expression of *RNF144A* (n=4). Welch's t-test. (D) Protein amount of *RNF144A* by western blot in variation of *RNF144A-AS1* levels. Lanes indicate biological replicates. (E) *RNF144A-AS1* level in GFP- or *SOX9*-transduced MSCs under different doses of TGF- $\beta$ 3 (n=6). Two-way ANOVA followed by Tukey post-hoc test ( $\alpha=0.05$ ) on the effect of *SOX9* overexpression ( $p < 0.0001$ ) and doses of TGF- $\beta$ 3 ( $p > 0.05$ ). The interaction between two tested factors (*SOX9* overexpression and TGF- $\beta$ 3 doses) was not significant ( $p > 0.05$ ). Groups of different letters are statistically different. *ns*: not significant.

**Figure 4:** *GRASLND* enhances chondrogenesis.

(A) Experimental timeline. (B,C) Biochemical analyses of day 21 MSC pellets (n=4). Welch's t-test. (D,E) qRT-PCR analyses of day 21 MSC pellets (n=5 in D; n=6 in E). Welch's t-test. (F) Representative histological images of day 21 MSC pellets. *COLII IHC*: collagen type II immunohistochemistry. *hOC*: human osteochondral control. Scale bar = 100  $\mu$ m. (B,D,F) Transgene ectopic expression of *GRASLND*. (C,E,F) CRISPR-dCas9-VP64 induced activation of *GRASLND*. *ns*: not significant ( $p > 0.05$ ).

**Figure 5:** *GRASLND* suppresses interferon type II signaling.

(A) Top 20 up- and down-regulated genes in *GRASLND* KD pellets compared to scrambled controls. (B) Gene ontology analysis of affected pathways. (C) Upregulated targets and related gene ontology terms and potential transcription factors. (D,E) Luciferase reporter assays on MSCs transduced with: (D) ISRE promoter element (n=3), or (E) GAS promoter element (n=3). Two-way ANOVA followed by Tukey post-hoc test ( $\alpha=0.05$ ). Groups of different letters are statistically different. (F) Biochemical assays on MSC-derived pellets cultured under 100 ng/mL of IFN- $\beta$  (n=4). (G) Biochemical assays on MSC-derived pellets cultured under 5 ng/mL of IFN- $\gamma$  (n=6). Welch's t-test. *ns*: not significant.

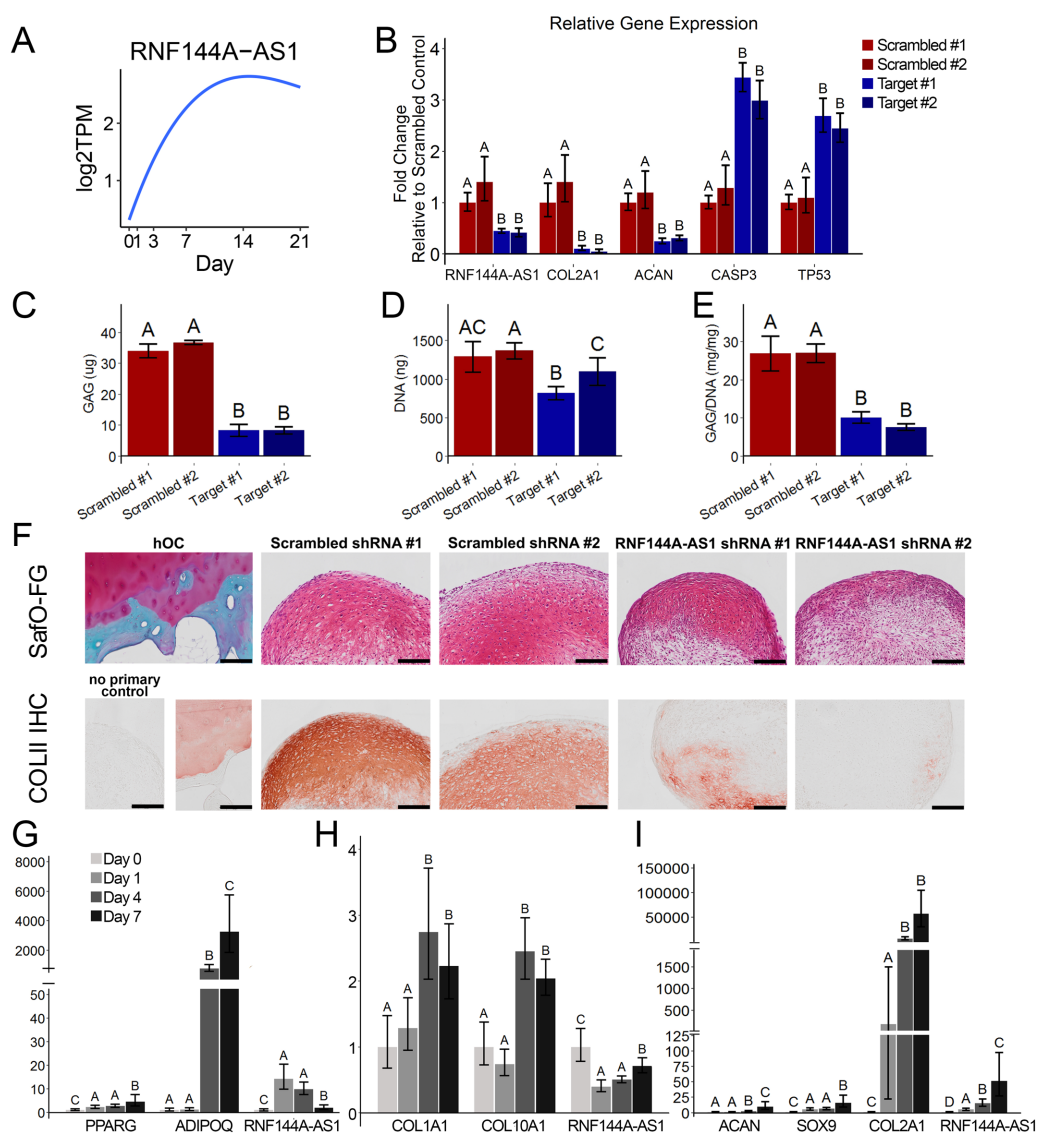
**Figure 6:** *GRASLND* enhances chondrogenesis in adipose-derived stem cells.

(A) Biochemical analyses (n= 5). (B) qRT-PCR analyses (n=6). (C) Representative histological images of day 21 ASC pellets. *COLII IHC*: *Collagen type II immunohistochemistry*. *hOC*: *Human osteochondral control*. Scale bar = 100  $\mu$ m. Welch's t-test. ns: not significant.

1

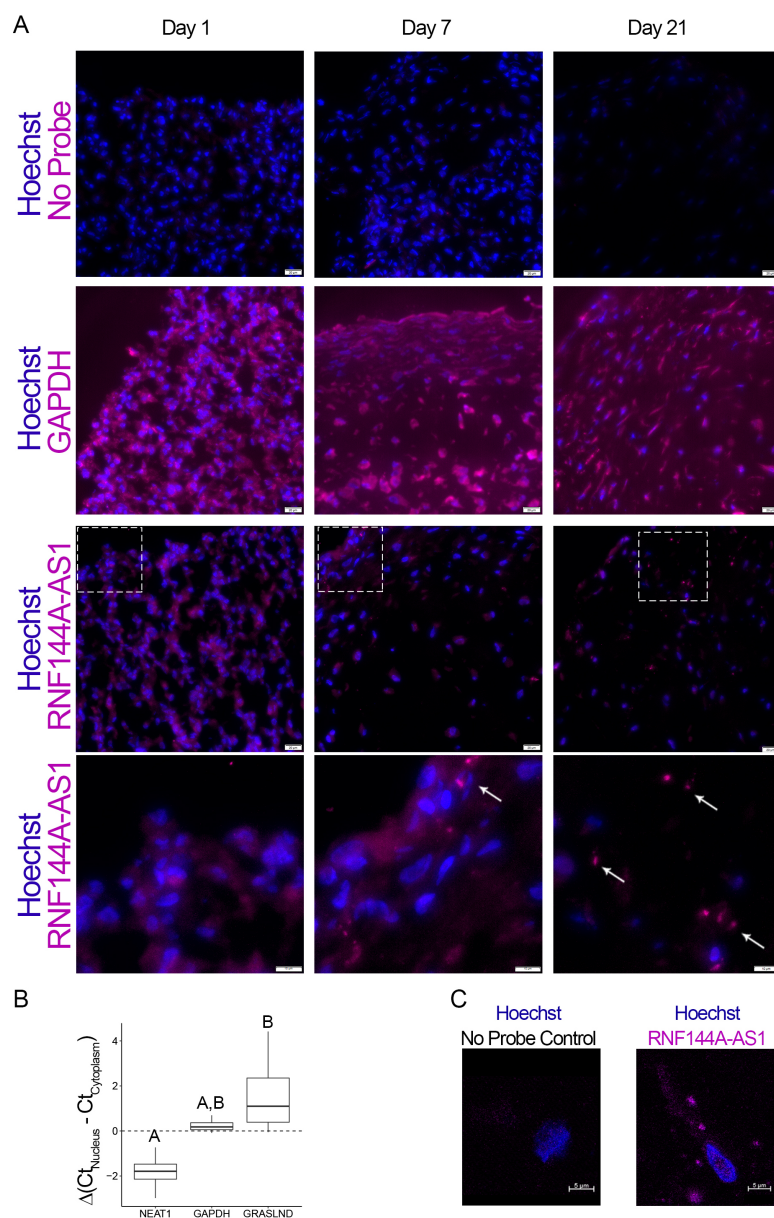


## 1 Figures



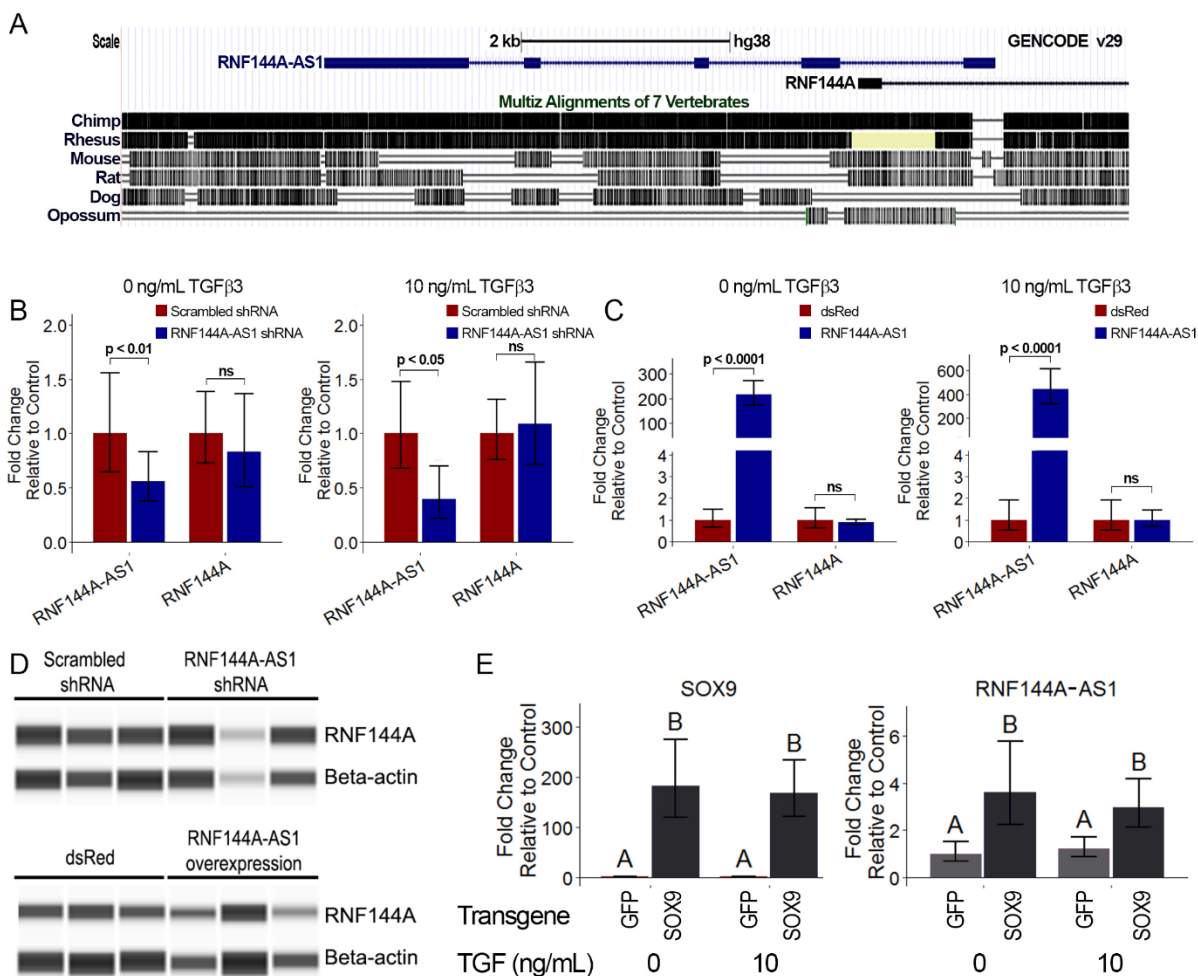
**Figure 1:** *RNF144A-AS1* is important and specifically upregulated in MSC chondrogenesis.

(A) Expression pattern of *RNF144A-AS1* in chondrogenesis (GSE109503 (36)). Log<sub>2</sub>TPM: log transformed value of transcripts per million (TPM). (B) Effect of *RNF144A-AS1* knockdown on chondrogenic, apoptotic, and cell cycle inhibition markers (n = 5). (C-E) Effect of *RNF144A-AS1* knockdown on pellet matrix synthesis (n = 5). (F) Representative histological images of day 21 MSC pellets. Scale bar = 200 μm. Safo-FG: SafraninO-Fast Green staining. COLII IHC: collagen type II immunohistochemistry. hOC: human osteochondral control. (G-I) qRT-PCR analysis of MSC samples cultured in (G) adipogenic condition (n=6), (H) osteogenic condition (n=6), (I) chondrogenic condition (n=3-4). One-way ANOVA followed by Tukey post-hoc test (α=0.05). Groups of different letters are statistically different from one another.



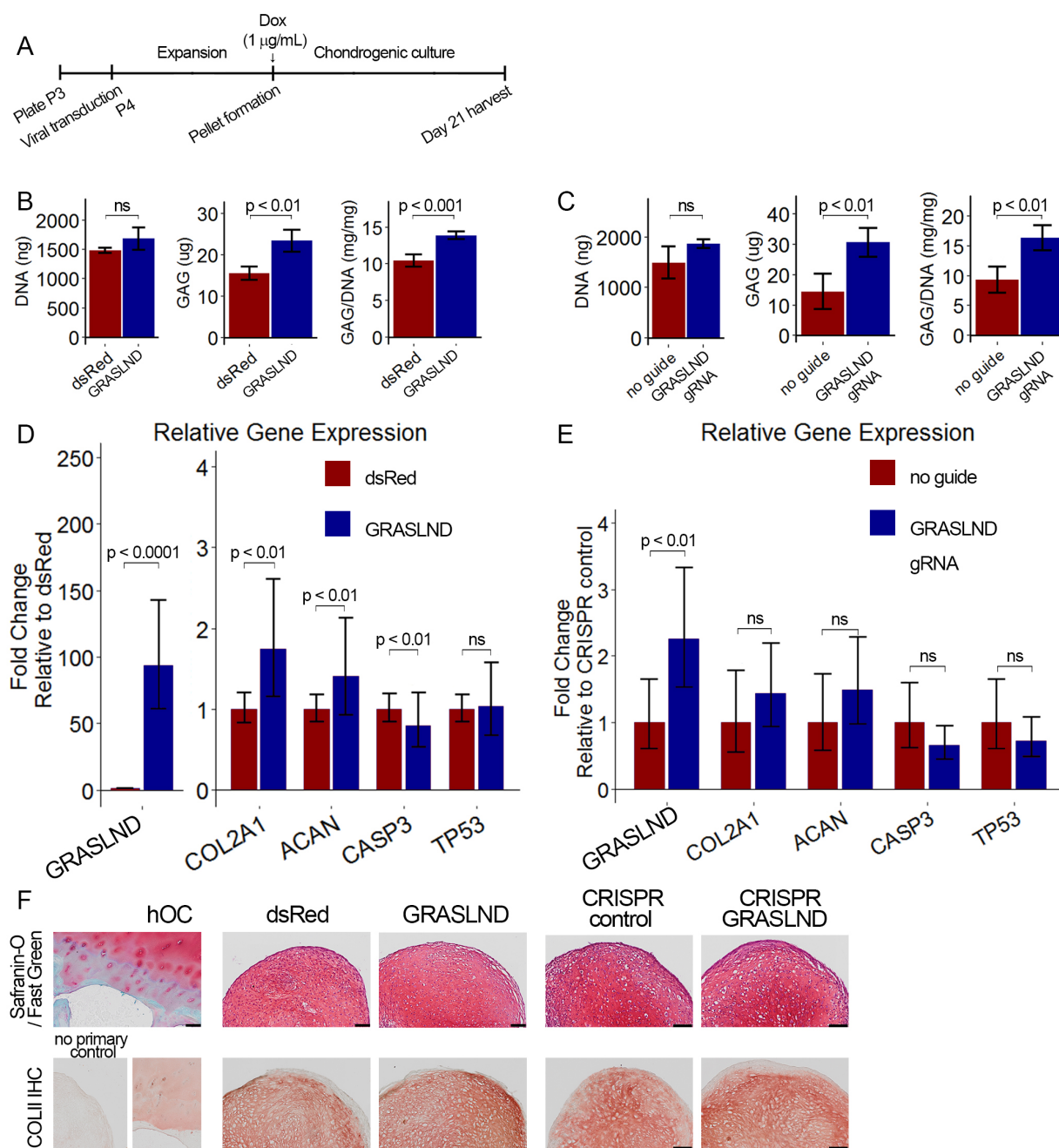
**Figure 2:** *RNF144A-AS1* is localized to the cytoplasm.

(A) RNA in situ hybridization of MSC-derived pellets at different time points during chondrogenesis. *GAPDH* and *RNF144A-AS1* probes were hybridized on separate slides. Scale bar = 20  $\mu$ m. (B) qRT-PCR of nuclear versus cytoplasmic fraction of day 21 MSC pellets (n=4). (C) Confocal microscopy on MSC-derived pellets. Scale bar = 5  $\mu$ m. One-way ANOVA followed by Tukey post-hoc test ( $\alpha=0.05$ ). Groups of different letters are statistically different from one another.



**Figure 3:** *RNF144-AS1* relationship to *RNF144A* and *SOX9*.

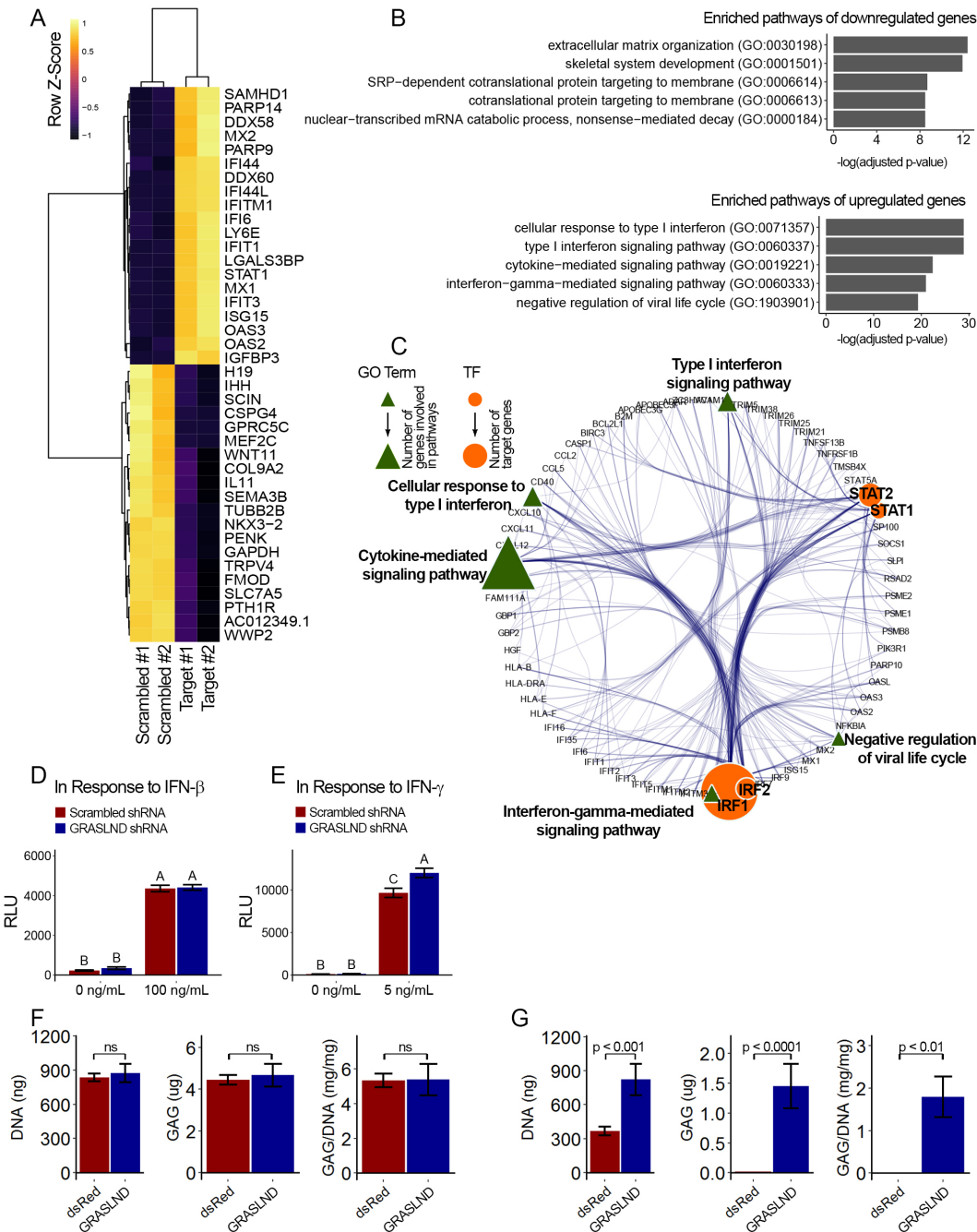
(A) *RNF144A-AS1* genomic location and conservation across different species. Data retrieved from UCSC Genome Browser. (B) Knockdown of *RNF144A-AS1* and expression of *RNF144A* (n=4). (C) Overexpression *RNF144A-AS1* and expression of *RNF144A* (n=4). Welch's t-test. (D) Protein amount of *RNF144A* by western blot in variation of *RNF144A-AS1* levels. Lanes indicate biological replicates. (E) *RNF144A-AS1* level in GFP- or *SOX9*-transduced MSCs under different doses of TGF-β3 (n=6). Two-way ANOVA followed by Tukey post-hoc test ( $\alpha=0.05$ ) on the effect of *SOX9* overexpression ( $p < 0.0001$ ) and doses of TGF-β3 ( $p > 0.05$ ). The interaction between two tested factors (*SOX9* overexpression and TGF-β3 doses) was not significant ( $p > 0.05$ ). Groups of different letters are statistically different. *ns*: not significant.



**Figure 4:** *GRASLND* enhances chondrogenesis.

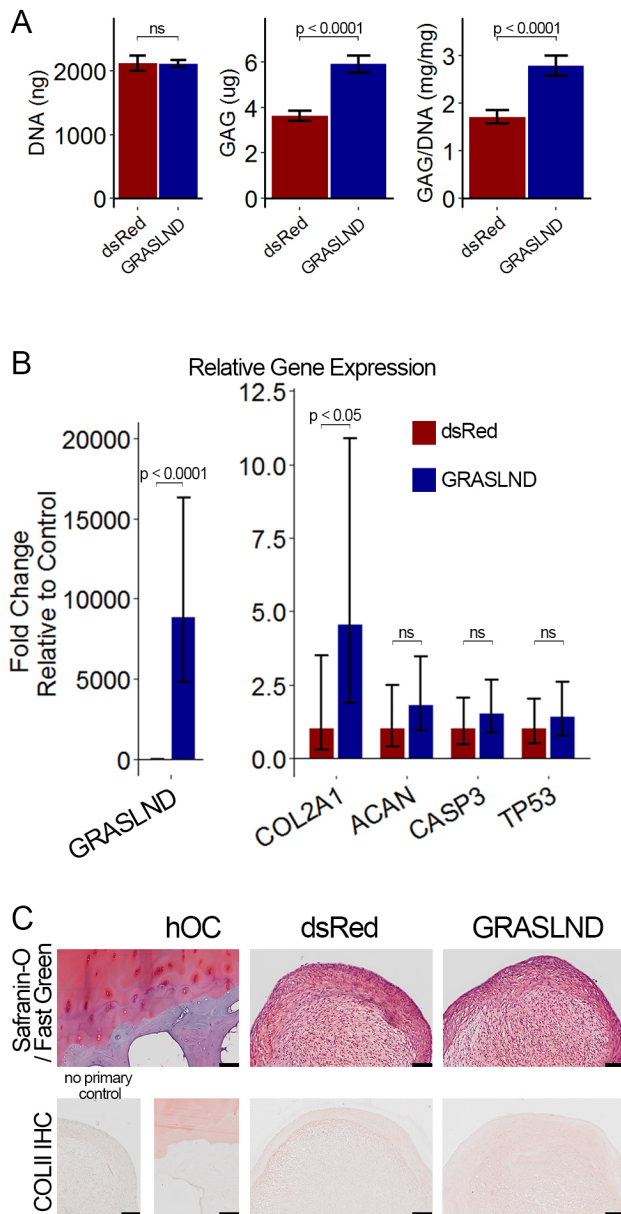
(A) Experimental timeline. (B,C) Biochemical analyses of day 21 MSC pellets (n=4). Welch's t-test. (D,E) qRT-PCR analyses of day 21 MSC pellets (n=5 in D; n=6 in E). Welch's t-test. (F) Representative histological images of day 21 MSC pellets. *COLII IHC*: collagen type II immunohistochemistry. *hOC*: human osteochondral control. Scale bar = 100 µm. (B,D,F) Transgene ectopic expression of *GRASLND*. (C,E,F) CRISPR-dCas9-VP64 induced activation of *GRASLND*. ns: not significant (p > 0.05).





**Figure 5: GRASLND suppresses interferon type II signaling.**

(A) Top 20 up- and down-regulated genes in *GRASLND* KD pellets compared to scrambled controls. (B) Gene ontology analysis of affected pathways. (C) Upregulated targets and related gene ontology terms and potential transcription factors. (D,E) Luciferase reporter assays on MSCs transduced with: (D) ISRE promoter element (n=3), or (E) GAS promoter element (n=3). Two-way ANOVA followed by Tukey post-hoc test ( $\alpha=0.05$ ). Groups of different letters are statistically different. (F) Biochemical assays on MSC-derived pellets cultured under 100 ng/mL of IFN- $\beta$  (n=4). (G) Biochemical assays on MSC-derived pellets cultured under 5 ng/mL of IFN- $\gamma$  (n=6). Welch's t-test. *ns*: not significant.

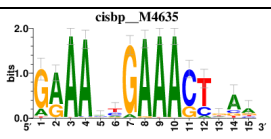
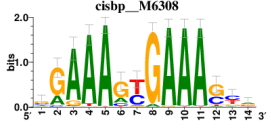
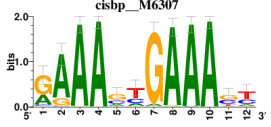
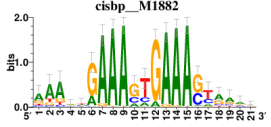
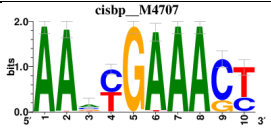


**Figure 6:** GRASLND enhances chondrogenesis in adipose-derived stem cells. (A) Biochemical analyses (n= 5). (B) qRT-PCR analyses (n=6). (C) Representative histological images of day 21 ASC pellets. COLII IHC: Collagen type II immunohistochemistry. hOC: Human osteochondral control. Scale bar = 100 µm. Welch's t-test. ns: not significant.

**Table 1: Long non-coding RNA candidates shortlist**

<b>Gene symbol</b>	<b>Gene name</b>	<b>ENSEMBL gene ID</b>	<b>Relationship to MSC chondrogenesis</b>	<b>Relationship to SOX9</b>
LOXL1-AS1	LOXL1 antisense RNA 1	ENSG00000261801	Correlated with MSC markers' expression	Downregulated upon SOX9 overexpression
MIR4435-2HG Gene synonym: MIR4435-1HG	MIR4435-2 host gene	ENSG00000172965	Correlated with MSC markers' expression	Downregulated upon SOX9 overexpression
HMGA2-AS1 Gene synonym: RP11-366L20.2	HMGA2 antisense RNA 1	ENSG00000197301	Correlated with MSC markers' expression	Upregulated upon SOX9 overexpression
RNF144A-AS1	RNF144A antisense RNA 1	ENSG00000228203	Correlated with chondrogenic markers' expression	Upregulated upon SOX9 overexpression

**Table 2: Top 5 enriched Cis-BP motifs and associated transcription factors for upregulated genes upon GRASLND knockdown**

Transcription Factor	Cis-BP motif*	Number of genes with enriched motifs / Number of upregulated genes
STAT2	 <p>cisbp_M4635</p>	212 / 817
IRF2	 <p>cisbp_M6308</p>	189 / 817
IRF1	 <p>cisbp_M6307</p>	220 / 817
IRF1	 <p>cisbp_M1882</p>	153 / 817
STAT1	 <p>cisbp_M4707</p>	262 / 817

\* Cis-BP: Catalogue of Inferred Sequence Preferences of DNA-Binding Proteins (79). Curated position weight matrices were retrieved from <http://motifcollections.aertslab.org>



## Supplemental Information

### I. Supplemental Figures

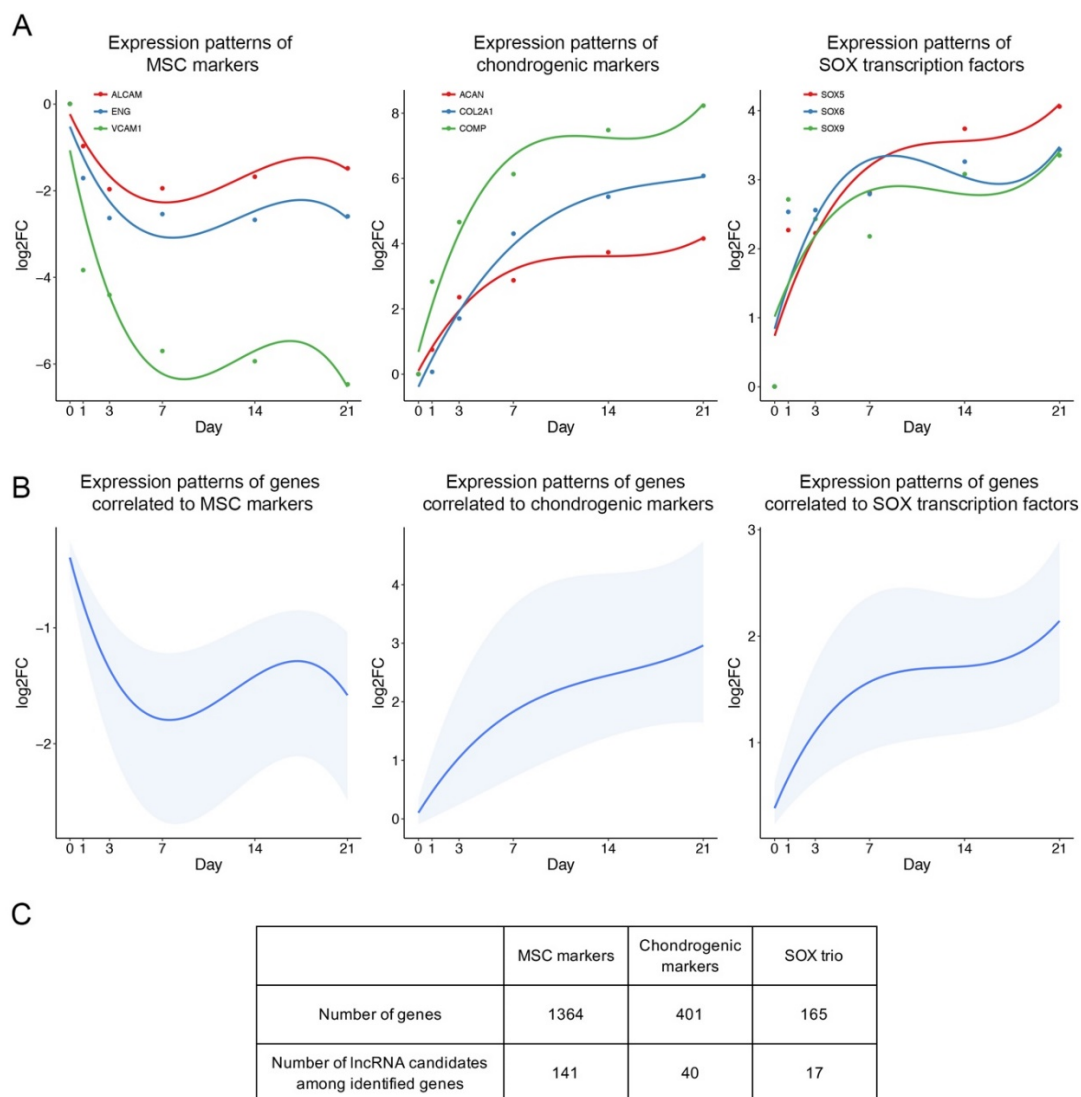


Figure S1: Identification of lncRNA candidates. LncRNAs whose expression patterns are correlated to crucial markers are of interest. (A) Expression patterns of previously identified MSC markers (left), chondrogenic markers (middle), and SOX transcription factors (right). Data retrieved from: GSE109503. (B) Expression patterns of correlated genes or lncRNAs (Pearson correlation > 0.9) to MSC markers (left), chondrogenic markers (middle),

and SOX transcription factors (right). Lower boundary: 25<sup>th</sup> percentile; upper boundary: 75<sup>th</sup> percentile; blue line: median; of correlated gene set. (C) Number of correlated genes and correlated lncRNAs.

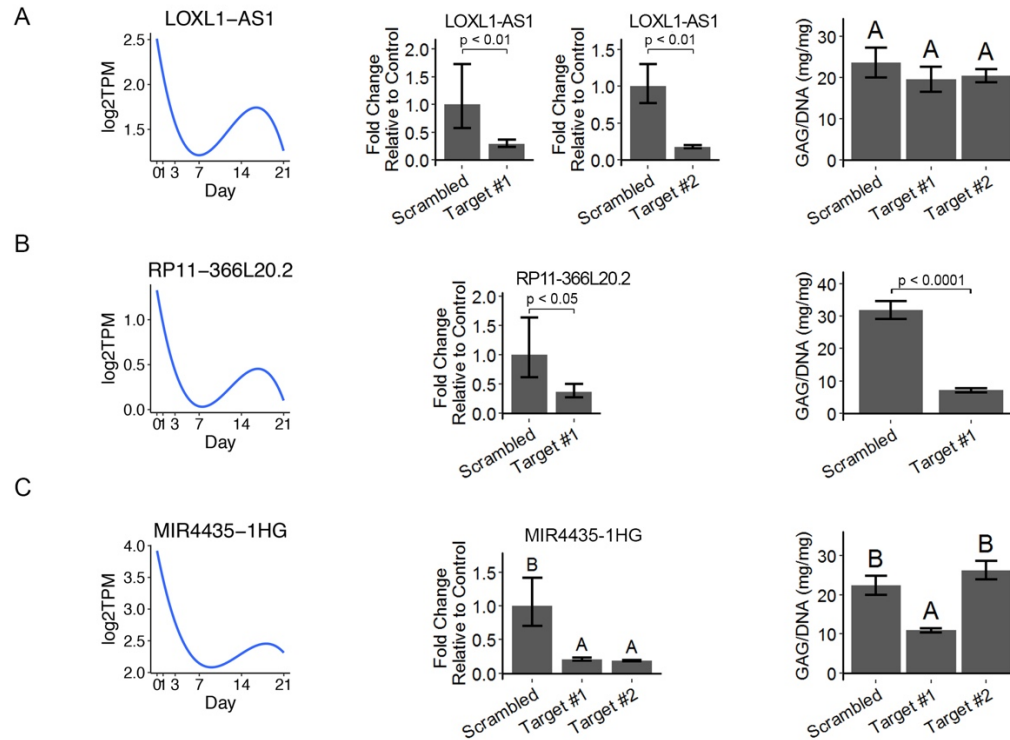


Figure S2: Functional validation of identified lncRNA candidates. **Left:** Expression pattern of candidates during chondrogenesis (GSE109503). Log<sub>2</sub>TPM: log-transformed value of transcripts per million (TPM). **Middle:** Efficiency of designed target shRNAs. Individual graphs indicate experiments on target number 1 and target number 2 were performed separately (n=3). Welch's t-test on log transformed fold changes for A-B. One-way ANOVA with Tukey post-hoc test for C ( $\alpha=0.05$ ). Groups of different letters are statistically different. **Right:** Quantitative analysis of synthesized GAG matrix normalized to DNA amount. (A) LOXL1-AS1 (n=4-5). One-way ANOVA with Tukey post-hoc test. Groups of different letters are statistically different. (B) RP11-366L20.2 (n=3-5). Welch's t-test. (C) MIR4435-1HG (n=3-

4). One-way ANOVA with Tukey post-hoc test. Groups of different letters are statistically different.

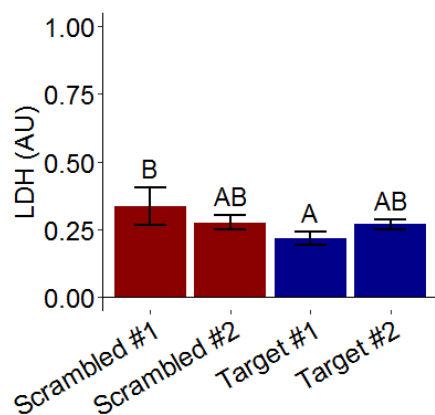


Figure S3: Cytotoxicity assay of target shRNAs. Cytotoxicity level was measured indirectly by the amount of released LDH (n = 4). One-way ANOVA followed by Tukey post-hoc test ( $\alpha = 0.05$ ). Groups of different letters are statistically different from one another.

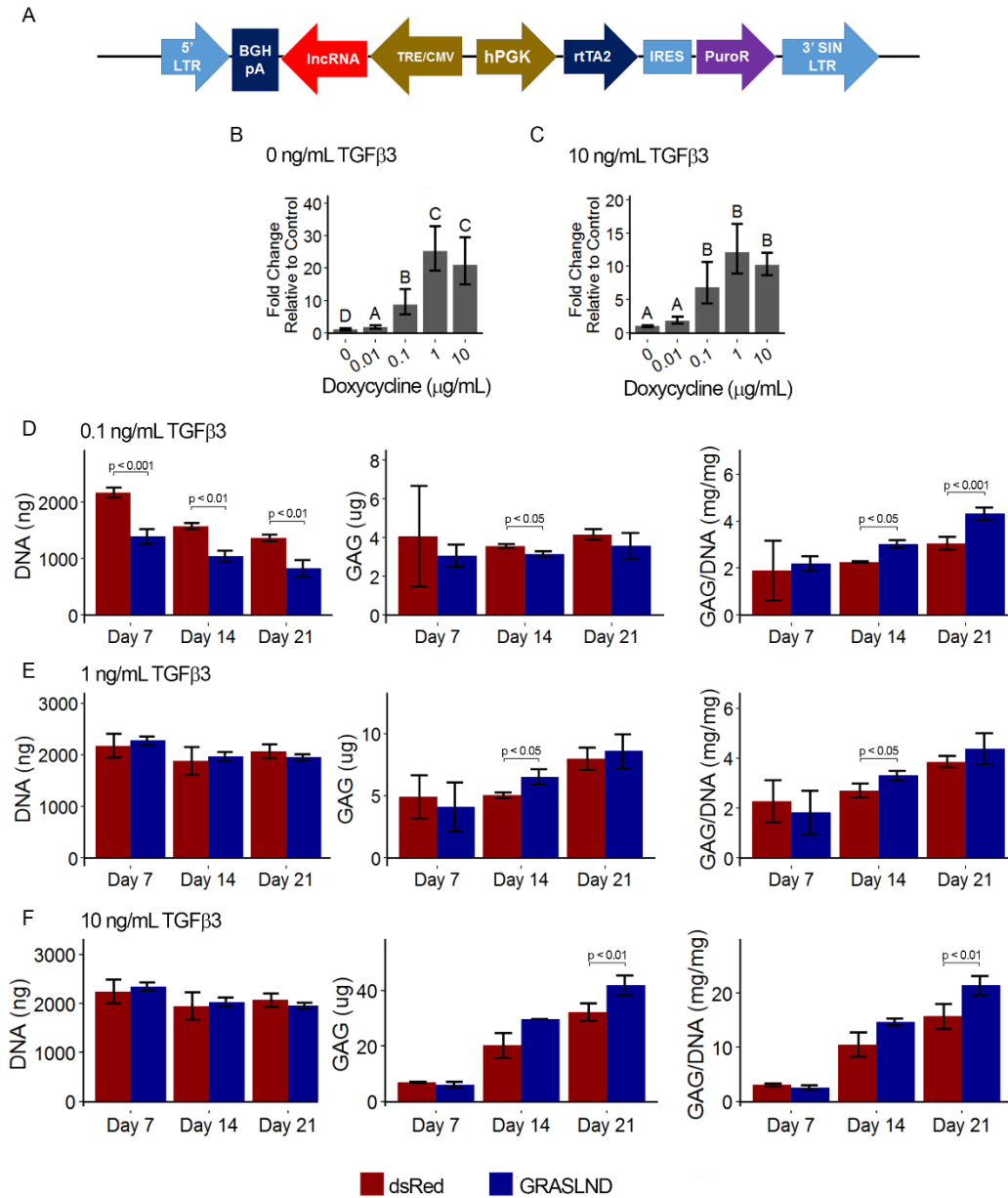


Figure S4: Effect of *GRASLND* overexpression across time points and tested doses.

(A) Overview of designed lentiviral backbone. *GRASLND* is driven under a Doxycycline inducible promoter, and poly-adenylated with BGHpA signal. (B-C) Relative expression of *GRASLND* under different doses of Doxycycline (Dox). Dox is most potent at 1  $\mu$ g/mL under both conditions of TGF- $\beta$ 3 (n=4). One-way ANOVA with Tukey post-hoc test ( $\alpha=0.05$ ). Groups of different letters are statistically different. (D-F) Biochemical analyses of MSC pellets

cultured under chondrogenic condition with different doses of TGF- $\beta$ 3 (n = 3-4). Welch's t-test. No bracket indicates the comparison is not significant. *LTR*: Long terminal repeat; *BGHpA*: Bovine growth hormone polyadenylation signal; *TRE/CMV*: Tet responsible element fused with the minimal cytomegalovirus promoter; *rtTA2*: Reverse tetracycline-controlled transactivator 2; *IRES*: Internal ribosome entry site; *PuroR*: Puromycin N-acetyl-transferase; *SIN*: Self inactivating.

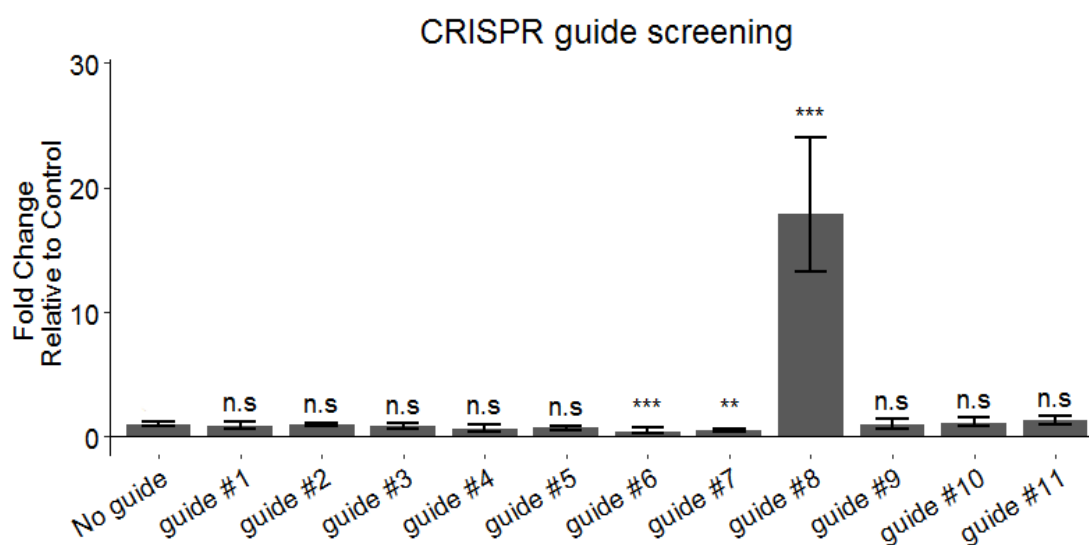


Figure S5: Synthetic guide RNA screening for efficient activation of endogenous *GRASLND*. Dunnett's test compared to "No Guide" control. ns: not significant. \*\* p < 0.01; \*\*\* p < 0.001.

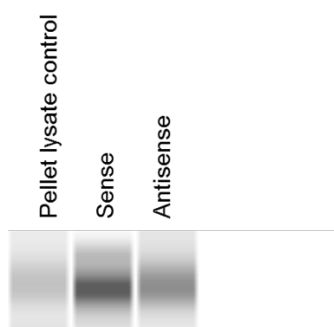


Figure S6: RNA pull-down followed by western blot confirmed EIF2AK2 as the binding partner of *GRASLND*.

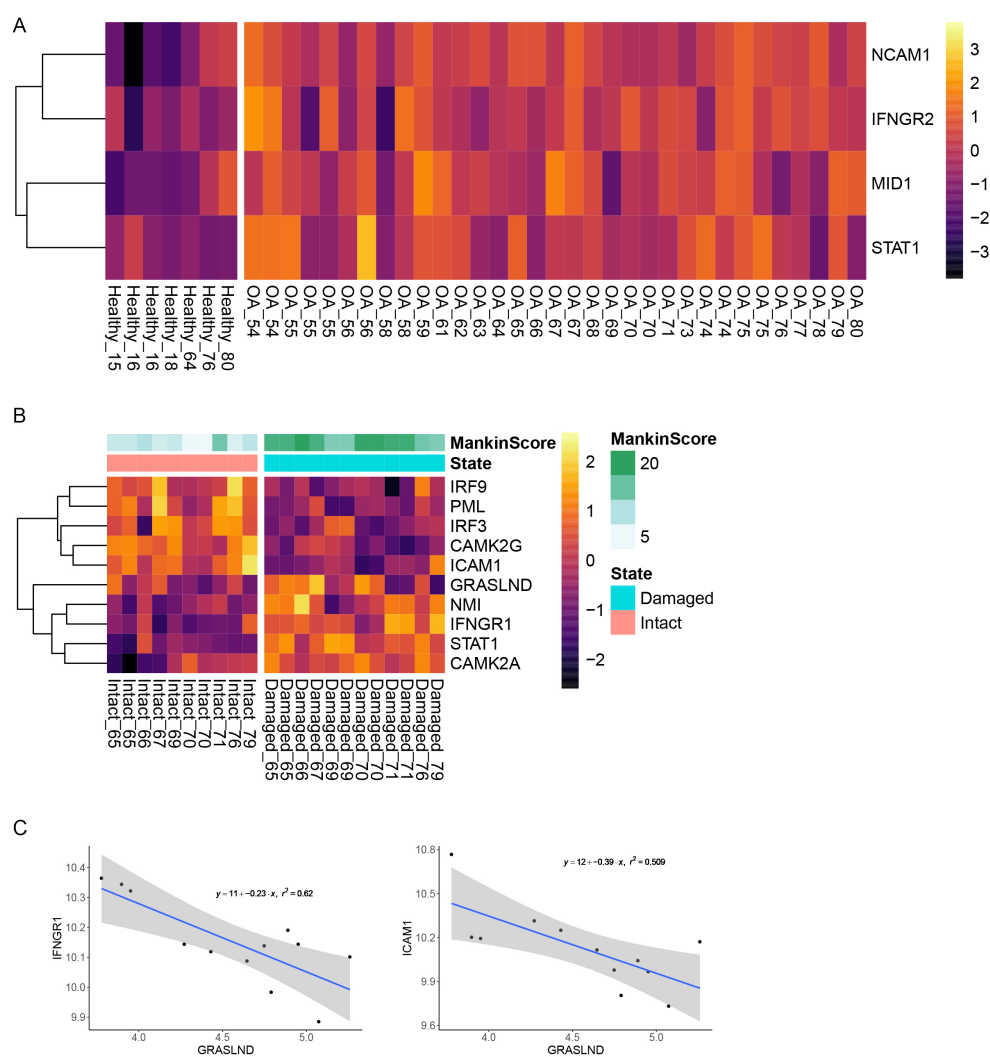


Figure S7: IFN signaling from other publicly available databases. (A) IFN signal was upregulated in OA patients. Samples are indicated as disease state followed by patients' age. (B) IFN was upregulated while *GRASLND* was downregulated in damaged cartilage. Samples are indicated as cartilage site followed by patients' age. (C) Inverse correlation between *GRASLND* and IFN-related genes.

## II. Supplemental Tables

Table S1: shRNA target sequences. 5' – sequence – 3'

Gene name	shRNA sequence
LOXL1-AS1	CAGAAGAGGTGCTCGATAAAT
	TGGGTACTTTATTTGCTATTA
MIR4435-1HG	ACAAGATGGTTAAACTCATTT
	CTATTCAGCAGACAATGATAA
RP11-366L20.2	GGTGATGTATGGCCATAAAT
RNF144A-AS1	TACAAAGGTGGCAAGATAAAT
	GGCAAGATAAATGACAATAAA

Table S2: Cloning primer sequences. 5' – sequence – 3'

BGHpA forward primer	TATCGATCACGAGACTAGCCTCGAGTCCATAGAGCCCACCGCAT
BGHpA reverse primer	CGCCGTGTAAACGCGTCGACTGTGCCTTCTAGTTG
Luciferase forward primer	GGCACAGTCGACGCGTTTACACGGCGATCTTGCC
Luciferase reverse primer	GCCCCGAATGCTAGCATGGAAGATGCCAAAAACATTAAG
CMV promoter forward primer	CATCTCCATGCTAGCATTGCGGGCCGCGGAGGC
CMV promoter reverse primer	CAACCCCGTGCGAATTCGATATCAATTTTATCGATCACGAGACTAGCCTCGAGTTTACC AC
dsRed forward primer	CAACTAGAAGGCACAGTCGACGCGTTTACAATTCGTGCTGCTTG
dsRed reverse primer	AGCCTCCGCGGCCCCGAATGCTAGCATGGATAGCACTGAGAAC
RNF144A-AS1 forward primer	CAACTAGAAGGCACAGTCGACGCGTCTTTCATTCAACAAATTTTTATGAAGTGCC
RNF144A-AS1 reverse primer	AGCCTCCGCGGCCCCGAATGCTAGCACGCCATTCTCCTGCCTC



Table S3: RNF144A-AS1 probe set sequences. 5' – sequence – 3'

Probe name	Probe sequence
Probe #1	GTTTCGTGGTCTTTTTCTAG
Probe #2	TAGGCAGGTCTCAGGATGTC
Probe #3	CTTCTGGAGGCCACCTAATG
Probe #4	CGGTGTAGGAATCAGGGGAG
Probe #5	GGTGAACAGACAGACTTTCC
Probe #6	AGATGTCCATTCCACCTTTT
Probe #7	TTCATCCTCTAGTGAGAGGC
Probe #8	CAGGCCTTTATGCAGAACGA
Probe #9	GTACTIONAACCAGGAACCTTCT
Probe #10	CCCTGAATCCTTCATTCATA
Probe #11	AACCATAATATCCCCCAGAT
Probe #12	AGACGTTACATTCCACATTC
Probe #13	TAGCACAGATGGGCTGAAGA
Probe #14	TGGCTTCTGGAATGAGATGA
Probe #15	TGTCTGCTCCTGAGAGAAGG
Probe #16	CTCTGGCAGGAAAGTCTTGT
Probe #17	TGTCTTATGTGGATGCTACT
Probe #18	GCTTGAAGACATCTCTGCAT
Probe #19	GCACTTTCTTTCTTGAAGTT
Probe #20	CAGTGCTGTGTTAAGTGACTION
Probe #21	ATGAGTAGTCACCTTCCATG
Probe #22	CCTTGTTCTCTAAGTTGCAG

Table S4: qRT-PCR sequencing primers 5' – sequence – 3'

Primer name	Primer sequence
r18S forward primer (endogenous control)	CGGCTACCACATCCAAGGAA
r18S reverse primer (endogenous control)	GGGCCTCGAAAGAGTCCTGT
GRASLND forward primer	AGGATTCAGGGGATGCACAG
GRASLND reverse primer	TGGGCTGAAGATGAGACGTT
COL2A1 forward primer	GGCAATAGCAGGTTACGTA
COL2A1 reverse primer	CTCGATAACAGTCTTGCCCC
ACAN forward primer	CACTTCTGAGTTCGTGGAGG
ACAN reverse primer	ACTGGACTCAAAAAGCTGGG
CASP3 forward primer	AGCGGATGGGTGCTATTGTG
CASP3 reverse primer	TCCAGAGTCCATTGATTCGCTT
TP53 forward primer	ACCTATGGAACTACTTCCTGAAAA
TP53 reverse primer	CCGGGGACAGCATCAAATCA
PPARG forward primer	AACGAGAGTCAGCCTTTAACGA
PPARG reverse primer	ATCCACGGAGCTGATCCCAA
ADIPOQ forward primer	GAGATCCAGGTCTTATTGGTCC
ADIPOQ reverse primer	ACACTGAATGCTGAGCGGTA
COL1A1 forward primer	TGTTTCAGCTTTGTGGACCTC
COL1A1 reverse primer	TTCTGTACGCAGGTGATTGG
COL10A1 forward primer	CATAAAAGGCCCACTACCCAAC
COL10A1 reverse primer	ACCTTGCTCTCCTCTTACTGC
SOX9 forward primer	ACCACCAGAACTCCAGCTC
SOX9 reverse primer	CACTGTGCTGGATATCAGACC
NEAT1 forward primer	ACAGCATTCTGTCTGCGAA
NEAT1 reverse primer	GACTTCAGGCTCCAGCCATT
GAPDH forward primer	TCACCAGGGCTGCTTTTAAC
GAPDH reverse primer	TGAAGACGCCAGTGGAC
RNF144A forward primer	CTGCTGACTCTGACATGCC
RNF144A reverse primer	CTGGTGTCTGCTGTGCTTA
LOXL1-AS1 forward primer	ACCAAAGCCAGGATCAGAGC
LOXL1-AS1 reverse primer	GAGGGTATCTTGCGGAGTGG
RP11-366L20.2 forward primer	TCTTGGGCCAACATGACACC
PR11-366L20.2 reverse primer	ACCTTCCTGGTTGGCTTTGT
MIR4435-1HG forward primer	TCCACAGCACATTTTTATTCAAGTC
MIR4435-1HG reverse primer	CTTCCTTGAGAATCTTGCTCCAAA

### III. Supplemental Materials and Methods

#### *Lentivirus production*

HEK 293T producer cells were maintained in 293T medium: DMEM-high glucose (Gibco), 10% heat inactivated FBS (Atlas), 1% Penicillin/streptomycin (Gibco). To produce lentivirus for pellet studies, HEK 293T cells were plated at  $3.8 \times 10^6$  cells per 10 cm dish (Corning) or at  $8.3 \times 10^6$  cells per 15 cm dish (Falcon) in 293T medium. The following day, cells were co-transfected by calcium phosphate precipitation with the appropriate transfer vector (20  $\mu$ g for 10 cm dish; 60  $\mu$ g for 15 cm dish), the second-generation packaging plasmid psPAX2 (Addgene #12260) (15  $\mu$ g for 10 cm dish; 45  $\mu$ g for 15 cm dish), and the envelope plasmid pMD2.g (Addgene #12259) (6  $\mu$ g for 10 cm dish; 18  $\mu$ g for 15 cm dish). Cells were incubated at 37°C overnight. The following day, fresh medium consisting of DMEM-high glucose (Gibco), 10% heat-inactivated FBS (Atlas), 1% Penicillin/streptomycin (Gibco), 4 mM caffeine (Sigma-Aldrich) was exchanged (12 mL for 10 cm dish; 36 mL for 15 cm dish). Lentivirus was harvested 24 hours post medium change (harvest 1), when fresh medium was exchanged again. 48 hours post medium change, harvest 2 was collected. Harvest 1 and harvest 2 supernatant were pooled, filtered through 0.45  $\mu$ m cellulose acetate filters (Corning), concentrated, aliquoted and stored at -80°C for future use.

To produce lentivirus for shRNA and gRNA screening, HEK 293T cells were plated at  $1.5\text{-}2 \times 10^6$  cells per well in a 6-well plate in DMEM-high glucose (Gibco), 10% heat inactivated FBS (Atlas). The following day, cells were co-transfected with 2  $\mu$ g of the appropriate transfer vector, 1.5  $\mu$ g of the packaging plasmid psPAX2 (Addgene #12260), and 0.6  $\mu$ g of the envelope plasmid (Addgene #12259) with Lipofectamine 2000 (ThermoFisher) following manufacturer's protocol. Harvest and storage were performed as described above.

For knockdown experiments, lentivirus was titered by determining the number of antibiotic resistant colonies after puromycin treatment. For overexpression experiments, lentivirus was

titered by measuring integrated lentiviral copy number in host DNA with qRT-PCR as previously described (1). Control and tested groups were targeted at similar MOIs.

### ***Lentivirus transduction***

Cells were plated at 4,500 cells/ cm<sup>2</sup> for one day and then transduced with appropriate lentivirus in expansion medium supplemented with 4 µg/mL polybrene (Sigma-Aldrich). Twenty-four hours post transduction, cells were rinsed once in phosphate buffered saline (PBS). Cells were cultured with fresh medium exchange every three days until future use.

### ***Cytotoxicity assay***

Seven days post viral transduction, medium was collected and the amount of lactose dehydrogenase (LDH) was measured as indirect output for cellular toxicity. Assays were performed following manufacturer's protocol (Promega). Absorbance signal was recorded at 490 nm with the Cytation 5 instrument (BioTek).

### ***RNA-seq library preparation***

Isolated RNAs were stored at -80°C and submitted to the Genome Technology Access Center at Washington University in St Louis for library preparation and sequencing on a HiSeq 2500 (2 x 101 bp). Libraries were prepared using TruSeq Stranded Total RNA with Ribo-Zero Gold kit (Illumina).

### ***RNA pull-down and mass spectrometry***

The full sequence of *GRASLND* transcript variant 1 (RefSeq NR\_033997.1) was synthesized by Integrated DNA Technologies, Inc, and cloned into the pGEM®-T Easy Vector System (Promega) using the EcoRV site. This served as a template for subsequent in vitro transcription using the Riboprobe® Combination Systems Kit (Promega), with spiked in biotin RNA labeling mix (Roche). Resulted biotinylated sense- and control antisense- transcripts of *GRASLND* were stored at -80°C until further processing.

Cell lysates from day 21 pellets were homogenized in mRIPA buffer (Cell Signaling) and centrifuged at 14,000 rpm for 15 minutes. The protein concentration of cell lysates was measured and adjusted to 2 mg/mL. Five hundred  $\mu$ L of total protein (1mg) were incubated with either 1.5  $\mu$ g of *GRASLND*-sense or antisense RNA transcripts tagged with biotin-16-UTP overnight (12 hours). Following incubation, the RNA-protein mixtures, and cell lysates (control) were incubated with 100  $\mu$ L of prewashed streptavidin beads for 3 hours at 4°C (Pierce™ MS-Compatible Magnetic IP Kit, Streptavidin, #90408). The streptavidin beads were then washed five times in 800  $\mu$ L of ice cold PBS. Beads were eluted twice, each with 30  $\mu$ L of SDS elution buffer containing 100 mM Tris/HCl pH 8, 4% SDS, 50mM DTT. The elution was either used for mass spectroscopy (Proteomics Core Facility, Washington University School of Medicine), or for Western blot (RayBiotech).

### ***Bulk RNA-seq analysis***

#### *Alignment and Read Assignment*

Demultiplexed raw sequencing files were generated by the Genome Technology Access Center at Washington University in St Louis. Reads were processed with trimmomatic-0.36 (2), aligned with STAR-2.6.0 (3), and counted with featureCounts/Subread-1.6.1 (4).

#### *Differential Expression Analysis*

Downstream differential expression analysis was performed using DESeq2-1.16.1 (5) ( $\text{abs}(\log_2 \text{fold change}) > 1$  and adjusted p-values  $< 0.05$ ).

#### *Gene Ontology Analysis*

Gene ontology analysis of dysregulated genes was performed with enrichR-1.0 (6, 7).

#### *Transcription Factor Identification*

Potential transcription factors were identified based on the presence of annotated DNA binding motifs with RcisTarget-1.0.2 (8). Annotation database for the motifs to human transcription factors were previously compiled and can be downloaded at

<https://resources.aertslab.org/cistarget/>. Cis-BP motifs were ranked by normalized enrichment score (NES), and the top five were reported in this paper.

### ***Identification of lncRNA candidates***

GSE109503 is the dataset that profiles transcriptomic changes of MSC chondrogenesis, composed of six time points (day 0, day 1, day 3, day 7, day 14, day 21) and three biological replicates. Raw sequencing files were downloaded from the GEO Omnibus, and processed as described above. Candidates were first restricted to those differentially expressed per day pair-wise ( $\text{abs}(\log_2 \text{ fold change}) > 1$  and adjusted p-values  $< 0.05$ ) and of detectable abundance (TPM  $> 1$  in more than 6 samples across the dataset). lncRNAs whose transcripts were not analyzed for transcript support level (ENSEMBL TSL) were also excluded. For the surviving genes, Pearson correlation analysis was then performed on mean expression per day. Candidates were identified as those with Pearson correlation values  $> 0.9$  to all three investigated markers (ALCAM, VCAM1, ENG for MSC markers; COL2A1, ACAN, COMP for chondrogenic markers; SOX5, SOX6, SOX9 for SOX transcription factors).

GSE69110 depicts the transcriptomic changes of fibroblasts in response to SOX9 expression levels. Raw sequencing files were downloaded from the GEO Omnibus, and processed similarly. Differentially expressed genes between two conditions (SOX9 overexpression versus GFP control) were then identified ( $\text{abs}(\log_2 \text{ fold change}) > 1$  and adjusted p-values  $< 0.1$ ). The shortlist of lncRNAs are the intersecting candidates between genes emerging from the above Pearson correlation analysis and dysregulated genes from this dataset.

### ***Microarray analysis***

Microarray processed data was downloaded from the GEO Omnibus and differential expression analysis was performed with limma-3.34.6 (9).

### ***Mass spectrometry analysis***

Scaffold-4.8.4 (Proteome Software Inc.) was used to validate MS/MS based peptide and protein identifications. Peptide identifications were accepted if they could be established at greater than 66.0% probability to achieve FDR less than 1.0% by the Scaffold Local FDR algorithm. Protein identification was accepted if they could be established at a greater than 95.0% probability and contained at least one identified peptide. Protein probabilities were assigned by the Protein Prophet algorithm (10). Proteins that contain similar peptides and could not be differentiated based on MS/MS analysis alone were grouped to satisfy the principles of parsimony. To identify differentially bound proteins, one tailed t-test was performed on sense samples compared to naked beads, and sense samples compared to antisense samples.

#### References

1. Sastry L, Johnson T, Hobson MJ, Smucker B, & Cornetta K (2002) Titering lentiviral vectors: comparison of DNA, RNA and marker expression methods. *Gene Ther* 9(17):1155-1162.
2. Bolger AM, Lohse M, & Usadel B (2014) Trimmomatic: a flexible trimmer for Illumina sequence data. *Bioinformatics* 30(15):2114-2120.
3. Dobin A, *et al.* (2013) STAR: ultrafast universal RNA-seq aligner. *Bioinformatics* 29(1):15-21.
4. Liao Y, Smyth GK, & Shi W (2014) featureCounts: an efficient general purpose program for assigning sequence reads to genomic features. *Bioinformatics* 30(7):923-930.
5. Love MI, Huber W, & Anders S (2014) Moderated estimation of fold change and dispersion for RNA-seq data with DESeq2. *Genome Biol* 15(12):550.
6. Chen EY, *et al.* (2013) Enrichr: interactive and collaborative HTML5 gene list enrichment analysis tool. *BMC Bioinformatics* 14:128.
7. Kuleshov MV, *et al.* (2016) Enrichr: a comprehensive gene set enrichment analysis web server 2016 update. *Nucleic Acids Res* 44(W1):W90-97.
8. Aibar S, *et al.* (2017) SCENIC: single-cell regulatory network inference and clustering. *Nat Methods* 14(11):1083-1086.
9. Ritchie ME, *et al.* (2015) limma powers differential expression analyses for RNA-sequencing and microarray studies. *Nucleic Acids Res* 43(7):e47.
10. Nesvizhskii AI, Keller A, Kolker E, & Aebersold R (2003) A statistical model for identifying proteins by tandem mass spectrometry. *Anal Chem* 75(17):4646-4658.